Age-based life-history parameters of the mesopelagic fish *Notoscopelus resplendens* (Richardson, 1845) in the Central Eastern Atlantic

A.N. Sarmiento-Lezcano[a,b], R. Triay-Portella[c], J.J. Castro[d], , U. Rubio-Rodríguez[b], J.G. Pajuelo[c,*]

[a] *Facultad de Ciencias del Mar, Universidad de Las Palmas de Gran Canaria, Edificio de Ciencias Básicas, Campus de Tafira, Las Palmas de Gran Canaria, 35017 Las Palmas, Spain.*

[b] *Instituto Politécnico Nacional, Departamento de Pesquerías y Biología Marina, CICIMAR-IPN, Av. Instituto Politécnico Nacional s/n. Col. Playa Palo de Santa Rita. La Paz, B.C.S., 23096. México.*

[c] *Applied Marine Ecology and Fisheries Group (EMAP). University Research Institute for Environmental Studies and Natural Resources (i-UNAT), Universidad de Las Palmas de Gran Canaria, Campus de Tafira, Las Palmas de Gran Canaria, 35017 Las Palmas, Spain.*

[d] *Grupo de Biodiversidad y Conservación, Instituto Universitario de Acuicultura Sostenible y Ecosistemas Marinos IU-ECOAQUA, Universidad de Las Palmas de Gran Canaria, Campus de Tafira, Las Palmas de Gran Canaria, 35017 Las Palmas, Spain.*

*corresponding author: jose.pajuelo@ulpgc.es, tel: +34 928454460

Abstract

The mesopelagic fish *Notoscopelus resplendens* is distributed mainly between 500 and 1000 m of depth during the day, with diel migration to surface waters at night (<90 m). Fish move during their diel migrations across different water masses, which show strong changes in temperature with depth that can reach 7 ºC in the first 300 m during the warm season. *N. resplendens* show a type of diel migration pattern of the "entire migrant", showing a clear day-night habitat separation, with peak abundance above 200 m at night. The difference between sexes in maximum size was 1.97 mm SL (84.36 mm, males; 82.39 mm females). The spawning season can be determined from December to March by back calculating the hatching date from daily growth increments. Age at first maturity was 1.7 year for males and 2.05 years for females. The sex ratio showed a predominance of males (1:0.67). Males were significantly more abundant than females in the 1-year age class. In the rest of the age classes, no significant differences were observed. A sexually dimorphic nature in relation to the position of the accessory luminous glands was observed. Three growth regions were observed in the otolith corresponding to different rates of deposition during fish ontogeny. Daily growth increments were calculated as validation of the annuli pattern. The pattern of the increment formation showed that each annulus has a unimodal distribution. The increment width decreases with age from 1 to 4 years. A strong relationship was found between both diameters of the otolith and length and

between otolith weight and age. Different growth models have been analysed to understand the growth of this species. Gomperzt and von Bertalanffy were the best models obtained and revealed differences in growth between sexes. The maximum age recorded was 4 years. The SL-TW relationship showed allometric positive growth. The natural mortality coefficient for the overall population derived from the age-frequency distribution was 0.579 $year^{-1}$. M obtained from the length converted catch curve was very similar at M=0.549 $year^{-1}$.

Keywords: Patchwork lampfish, growth pattern, hatched season, diel migration, age validation, natural mortality.

1. Introduction

Mesopelagic fish are the most abundant fish and indeed the most abundant vertebrates in the biosphere (Klevjer et al., 2016). These fish form one of the most characteristic features of the open ocean, the Deep Scattering Layer (DSL), which is present at a depth range between 200 and 1000 m (Catul et al., 2011; Irigoien et al., 2014; Olivar et al., 2017). The first global biomass estimate of fish that make up the DSL was 1000 million tons (Gjøsaeter and Kawaguchi, 1980), but this value could be underestimated, and it could be one order of magnitude higher (Irigoien et al., 2014). This high biomass implies that mesopelagic fish are an important part of the biological pump and a potential fishery resource (Longhurst and Harrison, 1989; Catul et al., 2011). However, these fish remain poorly investigated in relation to other components of the open ocean ecosystem, and there are many gaps in the knowledge of their biology and adaptations and even major uncertainties about their global biomass (Irigoien et al., 2014; Klevjer et al., 2016).

Mesopelagic fish cover thirty families, where most species are small-sized (usually between 2 and 15 cm in total length) with short life spans (Salvanes et al., 2001; Catul et al., 2011). Myctophidae is the main family within mesopelagic fish species, and it is present in all the world's oceans (Hulley, 1990; Catul et al., 2011). Myctophids are distributed throughout the water column, from superficial waters during the night to water exceeding 2000 m deep during the day but are more frequent between 200 and 1000 m deep as part of the Deep Scattering Layer (DSL) (Hulley, 1990; Catul et al., 2011). Due to the diel vertical migration occurring on a daily basis in the world's oceans performed by a large variety of zooplankton and micronekton species, mesopelagic fish play an important role as a link between plankton and top predators (Catul et al., 2011; Smith et al.,

2011: Olivar et al., 2017). Moreover, they are also very important in the flux of carbon transport to the deep ocean, as they comprise a significant fraction of the migrant biomass (Catul et al., 2011; Ariza et al., 2016). These mesopelagic fish are the most abundant species in the DSL of the Central Eastern Atlantic, and the genus *Notoscopelus* is the most representative group of myctophids in the area (Bordes et al., 2009).

The oceanographic conditions of the Canary Islands in the Central Eastern Atlantic are relevant and variable in depth and may have a remarkable influence over the distribution, abundance and growth of organisms. The Canary Islands are located in the Canary Current System, which is one of the 49 largest marine ecosystems in the world, characterized by their singular bathymetry, hydrography and productivity and their ability to support marine populations, which have adapted their feeding, reproductive and growth strategies (Hernández-León et al., 2007). The Canary Islands distinguish the Canary Current System from similar areas because the Canaries extend more than 600 km perpendicular to the general flow of the current. Therefore, the physical setting observed in the Canary region is quite different to that recorded in other main ocean current systems due to the mesoscale variability imposed by the islands (Barton and Arístegui, 2004; Hernández-León et al., 2007). Hydrologically, in the first 1000 m of depth, these islands are also characterized by special conditions derived from the presence of three water masses: the Eastern North Atlantic Central Water (ENACW), the Antarctic Intermediate Water (AIW) and the Mediterranean Water (MW), located at different depths and with characteristic thermohaline properties (Ríos et al., 1992; Hernández-Guerra et al., 2002, 2003). Additionally, the Canary Islands occupy a key position with respect to marine biogeochemical cycles because they are located in the boundary between eutrophic NW African upwelling waters and oligotrophic oceanic North Atlantic subtropical gyre waters (Wilke et al., 2009).

One of the most abundant species in the DSL of the *Notoscopelus* genus is *N. resplendens* (Richardson, 1985), which has a circumglobal distribution in mesopelagic and bathypelagic waters from tropical to temperate seas (Riede, 2004; Eschmeyer et al., 2018). This species shows the highest abundance levels in the Eastern Atlantic region along the African coast, including the Canary Islands (Nafpaktitis, 1975), in ecoregion 24, as described by Sutton et al. (2017) in a global biogeographic classification of the mesopelagic zone. Yatsu et al. (2005) also indicated that *N. resplendens* in the Kuroshio–Oyashio transition zone is one of the dominant components of mesopelagic fish.

In mesopelagic fish species, the estimation of age and growth is many times difficult. In some species, the age and growth have been estimated by reading their otoliths by means of annuli or daily growth depositions (Greely et al., 1999; Takagi et al., 2006; García-Seoane et al., 2015a). In

cold and temperate waters, both annual and daily increments have been described in mesopelagic species (Salvanes et al., 2001; García-Seoane et al., 2015a). However, in tropical and subtropical waters, only daily increments have been detected in mesopelagic species (Salvanes et al., 2001), due to a short life span and the lack of seasonality in water temperature and food availability (Salvanes et al., 2001).

Natural mortality has been noted as the most important parameter and the most difficult to obtain (Pauly, 1980). Errors in the estimation of natural mortality affect the estimations of models used in species assessments. An inaccurate estimate of natural mortality provided errors or bias in the cohort analysis (Mertz and Myers, 1997) or in the estimates of stock size using an age-structured model (Clark, 1999). Policy based on mortality is particularly sensitive to natural mortality parameters (Williams and Shertzer, 2003). Inaccurate estimates can lead to the mismanagement of exploited species (Beamish and McFarlane, 1995). Fish activity produces changes in natural mortality, producing an increment on many occasions. These increments in natural mortality may be part of the explanation of collapsed stocks (Jørgensen and Holt, 2013). In the last several decades, a wide variety of empirical techniques have been used to estimate M based in the fishing effort, age-frequency analyses, catch-curve methods or have been obtained from theoretical or empirically derived relations based on life history parameters (Kenchington, 2014). Natural mortality also has trophic and food web implications because natural mortality involves one species being eaten by another in a community and therefore describes flows of mass and energy in the ecosystems (Jørgensen and Holt, 2013). The knowledge of natural mortality in an unexploited population is also very important because fishing activity has been recognized as a driver of the evolution of life history traits expecting consequences for natural mortality (Jørgensen and Holt, 2013).

Despite the high abundance and the ecological importance that this species has in the food web of the Central Eastern Atlantic and in the flux towards the deep ocean, *N. resplendens* has not been studied in this area. The main goals were to estimate the age-based life-history parameters, deep distribution, and migration pattern of *N. resplendens* in an unexploited population in the Central Eastern Atlantic. Age and growth aspects and the estimation of the best model of growth for *N. resplendens* and the consistency of the ageing criteria used have been analysed. Age at first maturity and spawning period were also calculated. An estimate of the natural mortality from this unexploited population was also compared with the estimates derived from equations and methods that had been extensively used in stock assessments. Natural mortality derived from age-frequency analyses from this unexploited population and estimates obtained using published equations could

provide level of errors or the validation of some equations for this species. Such validation could be useful for population analyses where estimates are unavailable, or their accuracy is questionable.

2. Material and methods

2.1. Sample collection

The study was based on the analysis of specimens caught during four research cruises (January, March, May, and November) carried out by the B/E "La Bocaina" off the Canary Islands (Central Eastern Atlantic) in a depth range between 13 and 1577 m (Fig. 1). The specimens were caught with a commercial semi-pelagic trawl net, with a cod-end with a 5-mm mesh size, but in the last cruise, this was increased to 10.4 mm (Bordes et al., 1998). Fishing operations were monitored using acoustic telemetry with a net-sounder SCANMAR, which provided information on depth, the vertical and horizontal opening of trawl mouth, time and velocity. During each cruise, the salinity and temperature at the sea bottom were recorded using a XR-CTD sensor manufactured by LTD.

Captured specimens were labelled and stored in 70% ethanol for later analysis. Each fish was measured to the nearest 0.01 mm for standard length (*SL*) and total weight (*TW*, 0.01 g). Sex was estimated from 216 samples due to external body dimorphism by the position of the supracaudal luminous gland. When the presence of the glands could not be ascertained, the sex was classified as undetermined.

Sagittal otoliths were removed, cleaned, and stored dry for later age determination. All otoliths were photographed with a Canon EOS 6D digital camera coupled to a microscope. Measurements of the minimum diameter (*Omd*, μm) and maximum diameter (*OMd*, μm) of the otoliths (Fig. 2) and the radii of each annual increment (from the core to the outer edge of the increment) were obtained with a Fiji image process system (Schindelin et al., 2012). Each otolith was weighed (*OW*, mg) to the nearest 0.01 mg.

2.2. Data analysis

The age was determined by interpreting growth rings on the whole sagittal otoliths. All otoliths were aged twice by two independent readers, without prior information on length, sex or time of capture. In this comparison, the readings were done in a random order (Dwyer et al., 2003). Previous to these readings, burning and staining techniques and different liquids, which included

seawater, ethanol and glycerol were used to enhance the growth rings (McCurdy et al., 2002). There were no effects of the quality of the preparation technique on the enhancement of the growth ring. Therefore, water was adopted as the standard protocol. In addition, otoliths of a subsample of 20 individuals from Age-class 0 and 1 (10 by age class) were mounted on microscope slides and prepared by hand grinding and polishing on both sides to obtain transparent sagittal sections with the primordium reached. This otolith sections were examined and photographed with an optical microscope Nikon Eclipse 80i. Microincrements (daily growth increment) were observed at 1000× magnification under immersion oil. Microincrements were enumerated from the first distinguishable increment after the primordium, or 'core', to the otolith edge. The nomenclature of otolith microstructure was according to Giragosov and Ovcharov (1992). Three zones of growth increments were observed in the otoliths. These regions were described following García-Seoane et al. (2015a) for the validation of daily growth increments in myctophids. The regions observed within each sagitta were the larval zone, the postlarval zone and the postmetamorphic zone. The widths of the larval zone and postlarval zone were measured along the longest axis from the primordium to the dorsal edge following García-Seoane et al. (2015a). Microincrements were counted by two independent readers. When readers agreed in counts to within a 5% range of error, counts were accepted and averaged.

Two readers counted the microincrements within each zone two times for a 1-year class otolith. When both readers agreed (within a 5% of error) counts were accepted and averaged. When the counts differed, a third reading attempts was developed. If the counts differed by more than 5%, the otolith was rejected (García-Seoane et al., 2015a). The total number of microincrements was used to validate the age reading estimated in whole otoliths and the seasonal deposition of growth increments.

Annuli were counted from the core to the rostrum on the distal face of the whole otoliths along the antero-posterior axis using reflected light (Fig. 2). Readings were carried out using an OLYMPUS SZ60 stereoscopic microscope. To facilitate the reading, the dorsal side of the otoliths was polished with lapping film (12000 grit) (Takagi et al., 2006). Subsequently, to remove the calcareous remains, the samples were treated with 10% sodium hypochlorite for 24 hours and clarified with water prior to observation. The bias and precision of annulus counts were compared between readers using paired *t*-tests and age bias plots (Campana et al., 1995; Campana, 2001). Estimates of ageing precision were determined using the coefficient of variation (Chang, 1982).

The TW–SL relationship was estimated for males and females by means of a power equation by non-linear regression. The OMd-SL and Omd-SL relationships were estimated for males and

females using different non-linear models. The equality of the regressions was tested using an *F*-test. This test evaluated the null hypothesis of the equality of regressions estimated by sexes with a significance level of 5%, (α=0.05) and a critical value of $F_{0.05,1,>200}$=3.84 (Sachs, 1982; Sokal and Rohlf, 2012). Differences between the expected value from isometric growth and values of the regression coefficient (b) were compared using a *t*-test (Sachs, 1982). This test evaluated the null hypothesis H_0: b=3 in TW-SL relationship; and H_0: b=1 in OMd-SL and Omd-SL relationships, with a significance level of 5% (α=0.05) and a critical value of $t_{0.05,>200}$=1.97 (Sachs, 1982; Sokal and Rohlf, 2012). The equality in SL between males and females among age class was analyzed using two-way ANOVA. The sex ratio was estimated for the total sample and by age class. The Pearson chi-square goodness-of-fit test was used to evaluate the equality of frequencies between sexes.

Once all the rings on the otoliths were identified, the age was established by counting the number of seasonal increments on an annual basis. To establish the age class (number of calendar years after the birthday) to which a fish belonged, the number of annual increments was counted, and other information, such as the date of capture, the nature of the edge, and the main period of a seasonal increment formation and the birthday were taken into account (Morales-Nin and Panfili, 2002a). The species in the northern hemisphere are given a nominal birth date of 1st January (Morales-Nin and Panfili, 2002b). The difference between the date of capture and the birth date helps the reader to estimate the annual fraction elapsed since the last birth date, and the annual fraction was added to the number of complete translucent rings read in the otoliths to avoid any potential bias in growth estimates due to the differences in sampling dates (Gordoa and Molí, 1997). The average length and its standard deviation were also calculated for each age class.

Length-at-age was described using the von Bertalanffy growth function, the seasonalised von Bertalanffy growth function, the Schnute growth equation, and the Gompertz growth model (Pitcher and Macdonald, 1973; Ricker, 1973; Schnute, 1981). A nonlinear method of Levenberg-Mardquart's algorithm was used to estimate the growth parameters. The selection of the best growth model was based on the Akaike information criterion (AIC) which can be expressed as follows (Shono, 2000): $A_{IC} = \frac{RSS}{n} + \frac{2j(j+1)}{(n-j-1)}$, where *RSS* is the residual sum of squares, *n is* the number of observations, and *j* is the total number of estimated regression parameters. For model comparisons, the ΔA_{IC} and Akaike weights (A_w) were calculated. The model with the smallest A_{IC} value was selected as the best model (A_b). The ΔA_{IC} is the difference between the best model (A_b) and all other models (*i*), which is expressed as: $\Delta A_{ICt} = A_{ICt} - A_b \times A_w$, and represents the probability of choosing the correct model from the group of models used. Akaike weight is calculated for each model as: $A_w =$

$$\frac{\exp(-\Delta A_{IC}/2)}{\Sigma \exp(-\Delta A_{ICt}/2)}$$

Once the best model was determined, the growth parameters of males and females were compared using Hotelling's T^2 test (Bernard, 1981). The relationship between otolith weight (OW) and age were examined using the Gompertz model. A nonlinear method of Levenberg-Mardquart's algorithm was used to estimate the growth parameters

The natural mortality rate (M) was estimated using an age-catch curve from the unexploited populations and using a length-converted catch curve (Pauly, 1984) by means of the growth parameters estimated for the whole individuals. Additionally, the natural mortality rate was estimated using an empirical equation revised by Kenchington (2014).

3. Results

3.1. Size-structure

During the research cruises surveyed, 340 individuals (129 males, 87 females and 124 undetermined) of *Notoscopelus resplendens* were collected. The SL of the individuals ranged between 19.24 and 84.36 mm. The SL of males ranged between 28.39 and 84.36 mm and that of females from 30.45 to 82.39 mm. In the sample, males showed a higher mean size and mean weight than females. Student's *t*-test indicated that the null hypothesis was rejected for equality in the mean TW or for equality in the mean SL between the sexes (SL t=2.79>$t_{0.05,>200}$=1.97, p=0.006; TW t=2.931>$t_{0.05,>200}$=1.97, p=0.004). The difference between the sexes in maximum size and weight was 1.97 mm (2.39%) in SL and 0.31 g (5.96%) in TW. The Kolmogorov-Smirnov non-parametric *Z*-test showed that the null hypothesis of equality in the TW and SL distributions between sexes was rejected (TW: Z=1.96>$Z_{0.05}$=1.95, p=0.001; SL: Z=1.842>$Z_{0.05}$=1.96, p=0.002) (Fig. 3). The *F*-test for TW–SL relationship between the sexes indicated that the null hypothesis of equality of the two regressions estimated was retained (F=2.17>$F_{0.05,1,>200}$=3.89, p=0.1423). A *t*-test showing that null hypothesis of equality in the regression coefficient H_0: b=3 was rejected for all individuals (allometric positive, t=3.61>$t_{0.05,>120}$=1.97, p=0.0005), being isometric for males and females (t=1.85<$t_{0.05,>80}$=1.97, p>0.068).

The sex ratio showed a predominance of males (1:0.67), and the Pearson chi-square goodness-of-fit test indicated that the null hypothesis of the equality of sex frequencies was rejected (χ^2=8.167, p=0.004). Males were significantly more abundant than females in the 1-year age class (χ^2=20.25, p<0.0001). However, in the rest of the age classes, no significant differences were observed (χ^2<0.80,

265 p>0.371).

266

267 3.2. Depth distribution and temperature

268

269 In January, the coldest month, 36.4% of the individuals were caught during the night between
270 40 and 64 m in depth, and 63.6% were caught during the day at depths from 503 to 610 m. The
271 vertical diel migration in this period comprised a temperature range, at least from the 500-m
272 depth, of 6 ºC. In March, 87.7% of the individuals were caught during the night between 54 and 139 m
273 in depth, and 12.1% from 464 to 1577 m in depth during the day, with a diel temperature range of 7.5
274 ºC. In April, 95.5% of the individuals were caught at night between 40 and 66 m in depth, and
275 4.5% were caught during the day, and the diel range of temperature from 526 to 591 m was 8 ºC. In
276 November, 83.3% of the individuals were caught at night between 31 and 90 m in depth, and
277 16.7% were caught during the day from 606 to 924 m. The diel vertical migration comprised a
278 temperature range of 6.5 ºC. The diel maximum range of temperature from 500 m in depth was
279 reached in September with a value of 11 ºC (Fig. 4).

280

281 3.3. Otolith analysis

282

283 Otoliths have elliptic shape, with crenate margins (Fig. 2). The convex proximal face has a
284 groove, the sulcus acusticus. The distal face is relatively flat. The sulcus acusticus presents a sulcus
285 positioned on the midline of the otolith, with an ostium opening in the anterior margin of the otolith
286 and with tubular and short cauda closed far away from the posterior margin. The ostium is tubular
287 and longer than the cauda. The anterior region presents a broad and peaked small rostrum. The
288 antirostrum is small and narrow, and the excisura is wide, with a shallow acute notch. The posterior
289 region is round. Annuli were clearly differentiated under reflected light on a black background, with
290 the opaque rings milky in appearance and the translucent rings relatively transparent.

291 The otolith maximum diameter (OMd) ranged between 1469 and 4010 μm, and the otolith
292 minimum diameter (Omd) ranged between 1099 and 2605 μm. The relationships between OMd or
293 Omd and the SL were well described by a power function (Fig. 5). The *F*-test for OMd-SL and Omd-
294 SL relationships between sexes showed that the null hypothesis of the equality of the two regressions
295 estimated was rejected only in the OMd-SL case (OMd: F=4.857>$F_{0.05,1,>75}$=4.00, p<0.035). A *t*-test
296 showed that null hypothesis of equality in the regression coefficient (isometry) was rejected in all
297 cases.

The pattern of the increment formation is presented in Fig. 6, which shows that each annulus has a unimodal distribution. The increment width decreases with age from 1 to 4. As expected, increment widths are evidence of a decreasing growth rate of the otolith with increasing age.

The daily growth increments on 20 otoliths (age class 0 and 1) validate that only one annulus is formed for each 365 daily increments, being formed by one opaque and one translucent ring (Fig. 7). The number of increments in the larval zone was 35±3.9. The mean number of increments in the postlarval zone was 23±7.3, even though the width of the postlarval region was longer than larval zone (Fig. 8). The postmetamorphic region showed microincrements from the postlarval zone to the otolith edge, forming a set of opaque and translucent zones.

Taking into account the catch date of each individual of age-class 0 and 1, the spawning season can be located from December to March by back calculating the hatching date. Additionally, from the date of capture of each individual, the rate of opaque edge increased from January (15%) and March (47%) to May (79%), decreasing in November (43%). The period of formation of the translucent rings (observed under reflected light) coincided with the months in which the lowest values for seawater temperature in the first 200 m depth were reached, and the opaque rings coincided with the months in which the highest values were recorded.

There was no difference in ages estimated between the right and left otoliths (readers 1 and 2, CV=4.9 and CV=5.1; $p>0.05$) and between the two age readers (CV=4.66; $p>0.05$). The CV values were low, indicating the goodness of fit of the ageing procedure adopted and a reasonable level of consistency between readings. Age bias plots of ages estimated by the first reader compared to the second reader revealed no discrepancy between them (Fig. 9). Counts on otoliths were also compared between readers using a paired *t*-test for each age category. The values of the matched pair of *t*-tests revealed that there were no significant differences between the ages determined by the two readers ($t<1.135$; $p>0.257$).

3.4. Age estimation

Up to four annual marks were visible in the pooled otoliths sampled. Zero- and one-year-old fish were the dominant age classes, and only 36.76% of fish were two years old or older (Table 1). Over 49% of the growth was achieved by the end of the first year. By the end of the second year, fish had attained 75% of the maximum length observed. Age estimates ranged between 0 and 4 years for males and females (Table 1). A two-way ANOVA comparing the differences in SL between males and females among age classes showed significant differences for the factors of age classes

331 ($F_{0.05,4,>200}$=358.447, p<0.0001) and sex ($F_{0.05,2,>200}$=6.479, p=0.002), as well as for the interaction
332 effect ($F_{0.05,5,>200}$=3.215, p=0.008).
333
334 3.5. Growth models
335
336 The four models used gave good fits to the length-at-age data (Table 2). For males and females,
337 the Gompertz model was the best of the growth models fitted with an Akaike weight (A_w) of 0.41
338 and 0.45 for males and females, respectively (Table 2). The von Bertalanffy model follows rather
339 closely (A_w=0.39) for males and females, revealing between these two model a very high degree of
340 uncertainty regarding the best model for fitting the length-at-age data of males. Other models, such
341 as the Schnute or seasonalised von Bertalanffy models gave much lower values of A_w, indicating that
342 they do not fit the length-at-age data well. The Gompertz and von Bertalanffy models provided the
343 best fit for males and females; therefore, both functions were used to construct the growth curves for
344 both sexes (Fig. 10). Hotelling's T^2 test indicated significant differences between the growth curves
345 of the two sexes (T^2 Hotelling-test, T^2=11.09>$T_0{}^2{}_{0.05}$=3.88; p=0.0011).
346 The otolith weight ranged from 0.211 to 6.323 mg. The relationship between otolith weight and
347 age was well described by the Gompertz model (Fig. 11). Hotelling's T^2 test indicated significant
348 differences between the growth curves of the two sexes (T^2 Hotelling-test, T^2=6.23>$T_0{}^2{}_{0.05}$=3.88;
349 p=0.0133).
350
351 3.6. Natural Mortality
352
353 The natural mortality coefficient for the overall population derived from the age-frequency
354 distribution was 0.579 $year^{-1}$. The value of M obtained from the length-converted catch curve using
355 von Bertalanffy growth parameters for the whole population ($L\infty$=96.70 mm; k=0.417 $year^{-1}$; t_0=0.04
356 year) was very similar at 0.549 $year^{-1}$, with a difference of -0.03 $year^{-1}$ (5.18%). Values derived from
357 empirical equations showed a wide range of values from 0.49 to 1.668 $year^{-1}$ (Fig. 12). Two
358 empirical equations showed differences lower than 1% and another two differences lower than 15%.
359 The rest of the empirical equations showed differences higher than 50%.
360
361 **4. Discussion**
362
363 Although biological aspects have been studied in several myctophid species, especially the

364 growth (i.e. Moku et al., 2001; Takagi et al., 2006; Battaglia et al., 2015; García-Seoane et al.,
365 2015a,b; Hosseini-Shekarabi et al., 2015), this study is the first approach to estimate the age, growth
366 and other age-based demographic parameters of *Notoscopelus resplendens*. Additionally, it must be
367 noted that in the growth studies on myctophids, only the von Bertalanffy growth model has been
368 applied. However, in the present work, different models have been analysed to understand the growth of
369 this species.

370 Some myctophid species show a sexually dimorphic nature in relation to the position of the
371 accessory luminous glands (Catul et al., 2011), which has also been observed for *N. resplendens*.
372 Another frequent dimorphism pattern in myctophids is related to the size; males are markedly smaller
373 than females at maximum size (Catul et al., 2011). This, however, has not been observed for *N.*
374 *resplendens*, with similar maximum sizes for males and females.

375 The SL-TW relationship in *N. resplendens* indicated allometric positive growth for all
376 individuals, similar to that reported in many other myctophid species (Battaglia et al., 2010;
377 Hosseini-Shekarabi et al., 2015), including the congeneric *Notoscopelus elongatus*, which showed
378 similar size and weight ranges (Battaglia et al., 2015).

379 Species of the Myctophidae family show great variability in the diel migration patterns that
380 may be related with life history stage, sex, latitude, hydrography, topography and season
381 (Nafpaktitis, 1982; Hulley, 1985; Sassa et al., 2004; Catul et al., 2011). From the four-diel migration
382 pattern described by Watanabe et al. (1999) of migrants, semi-migrants, passive-migrants and non-
383 migrants, *N. resplendens* can be classified as a complete migrant, showing a clear day-night habitat
384 separation, with peak abundance above 200 m at night. This pattern has also been described in other
385 myctophid species, such as *Symbolophorus californiensis*, *Tarletonbeania taylori*, *Diaphus theta*,
386 *Ceratoscopelus warmingii*, *Diaphus gigas* and *Notoscopelus japonicus* (Watanabe et al., 1999).
387 Yatsu et al. (2005) indicated that *N. resplendens* in the Kuroshio-Oyashio transition zone ascended to
388 the upper 100 m layer at night, where this mesopelagic species concentrated at depths of 20-80 m.
389 Although some individuals of the population remain in the daytime habitat at night where they were
390 caught, the clear higher abundance in shallow waters and the absence of a separation in the depth
391 distribution of migratory and non-migratory individuals excluded the semi-migrant pattern
392 (Watanabe et al., 1999).

393 The relationships between fish length and otolith size contributes to provide a baseline for
394 trophic studies on predators for the estimation of biomass and size of prey items, which is the first
395 step in trophic or dietary works (Battaglia et al., 2015). The estimation of *N. resplendens* biomass as
396 prey from the otolith size helps to determine the importance of this species for top depredators in the

area and provides information on its role in the marine food web (Battaglia et al., 2010, 2015).

The daily deposition of microincrements may be different in different seasons, mainly in the cold season, when the otolith growth rates are lower (Mosegaard et al., 1988). Several authors for different myctophid species have noted that increment formation and growth apparently ceased at temperatures lower than 5 ºC (Kawaguchi and Mauchline, 1982; García-Seoane et al., 2015a). This suggests that temperature has an important effect on the growth rate and on increment deposition, and deposition may be disrupted in very low temperature conditions (García-Seoane et al., 2015a). In the Central Eastern Atlantic, *N. resplendens* is distributed mainly between 500 and 1000 m in depth during the day, with diel migration to surface waters at night. During the winter (cold season), the thermocline is dissolved, making water column temperatures more homogeneous, with seawater temperatures in the first 300 m of depth fluctuating from 16 to 19 ºC. In the warm season, water column stratification occurs, with the presence of a strong thermocline reaching fluctuations in the first 300 m from 17 to 24 ºC. These water temperature variations at the depth where this fish moves during its diel migrations could be enough for the clearer fixation of daily growth increments. Diel migration from the deep waters to the surface crossing these temperatures conditions throughout the year suggests that the daily increment deposition on the otoliths of *N. resplendens* also occurs during the cold season, when growth decreases. Growth and its decrease during the cold season have also been observed for other deep fish species in the area (Lorenzo and Pajuelo, 1995, 1999; González et al., 2003; Pajuelo et al., 2008, 2011). Additionally, during this daily migration, from 1000 to 10 m in depth, individuals must cross different water masses that also have strong influences over the distribution, abundance and growth of organisms (Hernández-León et al., 2007; Pajuelo et al., 2015). During the diel migration, individuals must cross through the Eastern North Atlantic Central Water mass and the Mediterranean and Antarctic Intermediate Water masses, with thermohaline values of temperature of 7-11 °C (Antarctic Intermediate), and salinity values for the Mediterranean water >35.3 psu (Ríos et al., 1992; Hernández-Guerra et al., 2001, 2002, 2003; Machín et al., 2006). Additionally, at the end of the Eastern North Atlantic Central Water mass that occurs at approximately 700 m in depth, the lower thermocline starts, corresponding with values of 11 ºC temperature and 35.5 psu in salinity (Hernández-Guerra et al., 2001; Machín et al., 2006). These changes in salinity and mainly in temperature result in the presence of density and thermal barriers for the vertical distribution of fauna (Pajuelo et al., 2015, 2016). However, myctophids are capable of crossing density gradients, such as thermoclines and haloclines, or wide hypoxic layers (Nafpaktitis and Nafpaktitis, 1969; Sassa et al., 2004; Catul et al., 2011; Olivar et al., 2017). This capability is because this species play an important role in oceanic energy dynamics, forming a link in the food

web between primary and tertiary consumers (Cherel et al. 2010; Catul et al., 2011). It also represents a pathway for the export of organic carbon between the surface and the deep ocean through diel vertical migration (Moku and Kawaguchi, 2008).

In the Central Eastern Atlantic, the changes in salinity and temperature with depth have a high influence on fish physiology during its vertical migration, and these factors produce the deposition of very clear daily growth increments. This influence in the deposition of microincrements has been recorded for other myctophid species (Linkowski et al., 1993; Linkowski, 1996; García-Seoane et al., 2015a) and for other deep fish species in the Central Eastern Atlantic (Lorenzo and Pajuelo, 1995, 1999; González et al., 2003; Pajuelo et al., 2008, 2011). These growth increments have been useful and used on many occasions to estimate age and growth in myctophid species (Young et al., 1988; Gartner, 1991a; Linkowski et al., 1993; Greely et al., 1999; Takagi et al., 2006; Bystydzieńska et al., 2010; García-Seoane et al., 2015a). However, the studies of age and growth using annual deposition patterns and its validation with the microstructure are scarce (Giragosov and Ovcharov, 1992; Greely et al., 1999; Shelekhov, 2004; García-Seoane et al., 2015b).

The three growth regions observed in the otolith of *N. resplendens* correspond with the same areas observed in other studies on myctophids (Gjøsaeter, 1987; Gartner, 1991a; Linkowski, 1991; Linkowski et al., 1993; Suthers, 1996; García-Seoane et al., 2015a; Hosseini-Shekarabi et al., 2015). These regions have been related to changes during fish ontogeny, such as body development, diel migrations, changes in habitat and diet, etc. (Linkowski, 1996; Mille et al., 2016). Increments in the larval and postlarval areas of *N. resplendens* were well defined and clearly visible. The results of the number of microincrement counts with a light microscope in the larval and postlarval zones were similar to those obtained in other studies on otoliths of myctophids (Gartner, 1991a; Giragosov and Ovcharov, 1992; Greely et al., 1999; Takagi et al., 2006; García-Seoane et al., 2015a). These results suggest that a light microscope resolution can be used to identify microincrements in larval and postlarval zones for *N. resplendens*. The first microincrement observed could be the hatch check. This check has also been recorded in other studies on myctophids species (Gartner, 1991b; Greely et al., 1999), and it has been assumed that they are formed during the first feeding (García-Seoane et al., 2015a). The time from hatching to the first microincrement (first feeding in larvae) is therefore unknown. The length of time is directly related with the time of yolk sac resorption, and this time amplitude can change with environmental temperature (García-Seoane et al., 2015a). In other myctophid species, this time of duration of the yolk sac varies from 3 to 5 days, when temperatures decrease from 25 to 21 ºC (Gjøsaeter and Tilseth, 1988; García-Seoane et al., 2015a).

The presence of different clear regions on myctophid otoliths have also been used to estimate

463 the chronology and the duration and of some life-history periods (Bystydzieńska et al. 2010; García-
464 Seoane et al., 2015a; Hosseini-Shekarabi et al., 2015). Larval zones correspond with the larval
465 growth, and the number of daily increments in this region indicates the time of the larval stage
466 (Gartner 1991b; García-Seoane et al., 2015a; Hosseini-Shekarabi et al., 2015). Larval stages of
467 myctophids are located in the epipelagic area at up to 200 m in depth, and they frequently do not
468 undergo diel migrations in depth (Moku et al., 2005; Catul et al., 2011). The numbers of
469 microincrements observed in the larval zone in otoliths of *N. resplendens* are similar to those
470 reported for *Benthosema pterotum* (Hosseini-Shekarabi et al., 2015). However, they are lower than
471 those recorded in other subtropical and tropical myctophid species, such as *Benthosema suborbitale*
472 (Gartner, 1991a), *C. warmingii* (Linkowski, 1997), or *Myctophum nitidulum* (Giragosov and
473 Ovcharov, 1992). During a metamorphic event, a migration occurs from the epipelagic to the
474 mesopelagic zone (Gartner, 1991b; Catul et al., 2011; García-Seoane et al., 2015a). During
475 migration, individuals move to deeper depths to adapt to their adult life in the mesopelagic zones,
476 after which some species start diel vertical migration (Sassa et al., 2004; Catul et al., 2011). This
477 migration and the changes in the environmental conditions of the habitat produce abrupt changes in
478 the metabolism of individuals who are recorded in the otolith in the postlarval region (García-Seoane
479 et al., 2015a). The numbers of increments observed in the postlarval zone of *N. resplendens* otoliths
480 appear to be in the ranges reported for *Benthosema glaciale* (García-Seoane et al., 2015a), *C.*
481 *warmingii* (Linkowski, 1997; Takagi et al., 2006), *Electrona antarctica* (Greely et al., 1999), *S.*
482 *californiensis* (Takagi et al., 2006) and *Tarletonbeania crenularis* (Bystydzieńska et al., 2010).
483 However, high variability has been reported in the larval and postlarval zones, with very low values
484 recorded, such as the case of *Diaphus kapalae* (Suthers, 1996) or *Lampanyctodes hectoris* (Young et
485 al., 1988). A low number of growth microincrements in postlarval zones in several myctophid
486 species have been related with a short metamorphosis period, because the larvae morphology does
487 not differ from the adults' morphology, and therefore, it is not an abrupt change in morphology and
488 does not take much time (Hosseini-Shekarabi et al., 2015).

489 The back calculation of the hatching date reveals that the spawning season of this species in the
490 Central Eastern Atlantic occurs from December to March, which is coincident with the result of the
491 spawning period recorded by Sarmiento-Lezcano (2016) and with the presence of *N. resplendens*
492 larvae in the water of the Canary Islands between January and March (Moyano and Hernández-León,
493 2011). The presence of larvae of *N. resplendens* was recorded when the water column was mixed and
494 characterized by low water temperature, medium salinity and medium-high values of the chlorophyll
495 concentration and mesozooplankton abundance (Moyano and Hernández-León, 2011). The hatching

496 period estimated was based on a low number of specimens, and a more extended spawning period
497 cannot be excluded. The size at first maturity was estimated in males at 51.78 mm SL and in females
498 at 55.08 mm SL (Sarmiento-Lezcano, 2016). These values correspond with early values of age at
499 first maturity of 1.7 years for males and 2.05 years for females, similar to those obtained for other
500 myctophids (García-Seoane et al., 2015b).
501 The growth parameters obtained in this study seems to be adequate because the predicted
502 asymptotic length value is slightly higher than the size of the largest fish sampled, and the growth
503 coefficient value indicated relatively fast attainment of maximal size. However, these parameters
504 indicated that *N. resplendens* grows slower than other species of the same genus, such as *N. elongatus*
505 in the Northeast Atlantic (Gjøsaeter, 1981). The obtained mean size by age indicated that *N.*
506 *resplendens* in the Central Eastern Atlantic reach 75% of its maximum size during the first year of
507 life. Nevertheless, the growth rate decreases with age.
508 The growth pattern described by von Bertalanffy's growth equation may be not the best
509 model for all mesopelagic fish species. Some show almost linear length increases with age and do
510 not tend to reach an asymptotic length throughout their lifetime (Salvanes et al., 2001). Others show
511 a slow down when their length increases as they become older but, do reach an asymptotic length
512 (Salvanes et al., 2001). The main causes of the seasonal cycles of growth are not well understood and
513 are known to be related to physiological changes induced by the influence of factors such as
514 temperature, diet and reproductive cycle (Pannella, 1980; Casselman, 1987). Myctophids, and in
515 particular, *N. resplendens*, carry out diel vertical migrations to feed; thus, it is possible that these
516 changes in depth will also translate into the seasonal formation of growth rings (Lai et al., 1996).
517 Discrepancies in the estimation of age in myctophids using microincrements and seasonal
518 increments have been reported for different species (Giragosov and Ovcharov, 1992; Linkowski,
519 1996; Greely et al., 1999; Shelekhov, 2004; García-Seoane et al., 2015a). These discrepancies can be
520 due to growth and deposition-disrupting processes during the winter due to low temperature.
521 However, in the case of *N. resplendens* inhabiting a high temperature environment, the daily
522 counting should be used to infer the true age of age-class-1 individuals. The daily characteristics of
523 growth increments in myctophid otoliths have been recorded in some species, mainly in tropical and
524 subtropical species (Gartner, 1991a; Suthers, 1996; Hayashi et al., 2001; Moku et al., 2001, 2005;
525 Hosseini-Shekarabi et al., 2015).
526 Myctophids are characterized by a short life span and a high mortality rates (Gjøsaeter and
527 Kawaguchi, 1980; Karuppasamy et al., 2008). The values obtained for *N. resplendens* confirm them.
528 The age catch curve and length-converted catch curve showed typical forms that justify the

estimation of a single value (Pauly, 1983). The natural mortality estimation for *N. resplendens* is slightly lower than that recorded for *Notoscopelus kroyeri* from the Northeast Atlantic (Gjøsaeter, 1981). This difference can be due to that the pressure of predators; the type and abundance of predators and their prey size preferences may be different among areas, even for the same species, as in the case of *B. glaciale* between Norway and Nova Scotia waters (Gjøsaeter, 1973, 1981; García-Seoane et al., 2015b). Additionally, the M values estimated are compatible with the M values recorded for the main deep predators present in the area, such as *Aphanophus carbo*, *Aphanophus intermedius*, *Promethychtys prometheus* or *Squalus megalops* (Lorenzo and Pajuelo, 1995, 1999; Pajuelo et al., 2008, 2011).

A specialist species has a life-history strategy that tends towards low productivity. Typical life-history characteristics include a large body size, a delayed age at sexual maturity, a long lifespan, and a low natural mortality and growth rate (Winemiller and Rose, 1992). In contrast, a generalist species will have a life-history strategy leaning towards the opportunistic use of resources. Therefore, generalists exhibit early maturity, a high growth rate, a small body size, and a short generation time, allowing for rapid recoveries of the population under unfavourable conditions and a high natural mortality and growth rate (Winemiller and Rose, 1992; García-Seoane et al., 2015b). To understand where *N. resplendens* fits in this life-history classification continuum, various life-history parameters such as maximum age, maximum size, growth rate, mortality, and age at maturity must be considered together (Pajuelo et al., 2008). In this context, the age-based life-history parameters of *N. resplendens* confirm that this species has a generalist strategy. This strategy, which is likely to be the general situation in myctophids, could make this species less prone to overexploitation (in a fishing activity scenario) due to a low reduction in surplus production (Pajuelo et al., 2008).

5. Acknowledgements

Thanks to Dr. Bordes and Dr. Barrera-Lujan to give us of biological material obtained during the cruises in the B/E La Bocaina.

6. References

Ariza, A., Landeira, J., Escánez, A., Wienerroither, R., de Soto, N.A., Røstad, A., Kaartvedt S.,Hernández-León S., 2016. Vertical distribution, composition and migratory patterns of acoustic scattering layers in the Canary Islands. J. Mar. Syst. 157, 82–91.

562 Barton, E.D., Arístegui, J., 2004. The Canary Islands coastal transition zone upwelling, eddies and
563 filaments. Prog. Oceanogr. 62, 67–69.
564 Battaglia, P., Malara, D., Romeo, T., Andaloro, F., 2010. Relationships between otolith size and fish
565 size in some mesopelagic and bathypelagic species from the Mediterranean Sea (Strait of
566 Messina, Italy). Sci. Mar. 74, 605–612.
567 Battaglia, P., Malara, D., Ammendolia, G., Romeo, T., Andaloro, F., 2015. Relationships between
568 otolith size and fish length in some mesopelagic teleosts (Myctophidae, Paralepididae,
569 Phosichthyidae and Stomiidae). J. Fish Biol. 87, 774–782.
570 Beamish, R.J., McFarlane, G.A., 1995. A discussion of the importance of aging errors, and an
571 application to Walleye Pollock: the world's largest fishery. In: Secor, D.H., Dean, J. M., and
572 Campana, S.E., (Eds.), Recent developments in fish otolith research. University of South
573 Carolina Press, Columbia, pp. 545–565.
574 Bernard, D.R., 1981. Multivariate analysis as a means of comparing growth in fish. Can. J. Fish. Aquat.
575 Sci. 38, 233–236.
576 Bordes, F., Almeida, C., Barrera, A., Carrillo, J., Castillo, R., Coca-Sáez, J., Gómez, J., Hansen,
577 K., Pérez, F., Ramos A., Uiblein, F., 1998. Prospección acústica y pesquera de los recursos
578 pelágicos en Lanzarote, Fuerteventura y Gran Canaria (Islas Canarias). Resultados de la
579 Campaña "Bocaina 1997". Viceconsejería de Pesca. Gobierno de Canarias.
580 Bordes, F., Wienerroither, R., Uiblein, F., Moreno, T., Bordes, I., Hernández-García, V., Caballero, C.,
581 2009. Catálogo de especies meso y batipelágicas. Peces, moluscos y crustáceos. Colectadas
582 con arrastre en las Islas Canarias, durante las campañas realizadas a bordo de B/E "La
583 Bocaina". Instituto Canario de Ciencias Marinas (ICCM), Agencia Canaria de Investigación,
584 Innovación y Sociedad de la Información-Gobierno de Canarias, Consejería de Agricultura,
585 Ganadería, Pesca y Alimentación, Viceconsejería de Pesca., 326 p.
586 Bystydzieńska, Z.E., Phillips, A.J., Linkowski, T. B., 2010. Larval stage duration, age and growth of
587 blue lanternfish *Tarletonbeania crenularis* (Jordan and Gilbert, 1880) derived from otolith
588 microstructure. Env. Biol. Fish. 89, 493–503.
589 Campana, S.E., 2001. Accuracy, precision and quality control in age determination, including a
590 review of the use and abuse of age validation methods. J. Fish Biol. 59(2), 197–242.
591 Campana, S.E., Annand, M.C., McMillan, J.I., 1995. Graphical and statistical methods for
592 determining the consistency of age determinations. Trans. Am. Fish. Soc. 124(1), 131–138.
593 Casselman, J., 1987. Determination of age and growth. The biology of Fish Growth, pp. 209–242.
594 Catul, V., Gauns, M., Karuppasamy, P.K., 2011. A review on mesopelagic fishes belonging to family

595 Myctophidae. Rev. Fish Bio. Fish. 21, 339–354.
596 Chang, W.Y., 1982. A statistical method for evaluating the reproducibility of age determination. Can.
597 J. Fish. Aquat. Sci. 39, 1208–1210.
598 Cherel, Y., Fontaine, C., Richard, P., Labat, J.P., 2010. Isotopic niches and trophic levels of
599 myctophid fishes and their predators in the Southern Ocean. Limnol. Oceangr. 55, 324–332.
600 Clark, W.J., 1999. Effects of an erroneous natural mortality rate on a simple age-structured stock
601 assessment. Can. J. Fish. Aquat. Sci. 56, 1721–1731.
602 Dwyer, K.S., Walsh, S.J., Campana, S. E., 2003. Age determination, validation and growth of Grand
603 Bank yellowtail flounder (*Limanda ferruginea*). ICES J. Mar. Sci. 60, 1123–1138.
604 Eschmeyer, W., Fricke, R., van der Laan, R., 2018. Catalog of Fishes, electronic version (3 January
605 2018). San Francisco, CA (California Academy of Sciences).
606 García-Seoane, E., Meneses, I., Silva, A., 2015a. Microstructure of the otoliths of the glacier
607 lanternfish, *Benthosema glaciale*. Mar. Freshw. Res. 66, 70–77.
608 García-Seoane, E., Fabeiro, M., Silva, A., Meneses, I., 2015b. Age-based demography of the glacier
609 lanternfish (*Benthosema glaciale*) in the Flemish Cap. Mar. Freshw. Res. 66, 78–85.
610 Gartner, J.V.J., 1991a. Life histories of three species of lanternfishes (Pisces: Myctophidae) from the
611 eastern Gulf of Mexico. Mar. Biol. 111, 11–20.
612 Gartner, J.V.J., 1991b. Life histories of three species of lanternfishes (Pisces: Myctophidae) from the
613 eastern Gulf of Mexico. Mar. Biol. 111, 21–27.
614 Giragosov, V.Y., Ovcharov, O.P., 1992. Age and growth of the lantern fish *Myctophum nitidulum*
615 (Myctophidae) from the tropical Atlantic. J. Ichtyol. 32, 34–42.
616 Gjøsaeter, H., 1987. Primary growth increments in otoliths of six tropical myctophid species. Biol.
617 Oceanogr. 4(4), 359–382.
618 Gjøsaeter, J., 1973. Age, growth, and mortality of the mygtophid fish, *Benthosema glaciale*
619 (Reinhardt), from Western Norway. Sarsia. 52(1), 1–14.
620 Gjøsaeter, J., 1981. Life history and ecology of the myctophid fish *Notoscopelus elongatus kroeyeri*
621 from the Northeast Atlantic. Fiskeridir. Skr. 17, 133–152.
622 Gjøsaeter, J., Kawaguchi, K., 1980. A review of the world resources of mesopelagic fish. FAO Fish.
623 Tech. Pap. 193: 1–151.
624 Gjøsaeter, J., Tilseth, S., 1988. Spawning behaviour, egg and larval development of the myctophid
625 fish *Benthosema pterotum.* Mar. Biol. 98, 1–6.
626 González, J.A., Rico, V., Lorenzo, J.M., Reis, S., Pajuelo, J.G., Afonso-Dias, M., Mendonça, A.,
627 Drug, H.M., Pinho, M.R., 2003. Sex and reproduction of the alfonsino *Beryx splendens* (Pisces,

628 Berycidae) from the Macaronesian archipelagos. J. Appl. Ichthyol. 19, 104–108.
629 Gordoa, A., Molí, B., 1997. Age and growth of the sparids *Diplodus vulgaris*, *D. sargus* and *D.*
630 *annularis* in adult populations and the differences in their juvenile growth patterns in the north-
631 western Mediterranean Sea. Fish. Res. 33(1-3), 123–129.
632 Greely, T., Gartner, J. Jr., Torres, J., 1999. Age and growth of *Electrona antarctica* (Pisces:
633 Myctophidae), the dominant mesopelagic fish of the Southern Ocean. Mar. Biol., 133, 145–
634 158.
635 Hayashi, A., Kawaguchi, K., Watanabe, H., Ishida, M., 2001. Daily growth increment formation and
636 its lunar periodicity in otoliths of the myctophid fish, Myctophum asperum (Pisces:
637 Myctophidae). Fish. Sci. 67, 811–817.
638 Hernández-Guerra, A., López-Laatzen, F., Machín, F., de Armas, D., Pelegrí, J., 2001. Water masses,
639 circulation and transport in the eastern boundary current of the North Atlantic subtropical
640 gyre. Sci. Mar. 65, 177–186.
641 Hernández-Guerra, A., Machín, F., Antoranz, A., Cisneros-Aguirre, J., Gordo, C., Marrero- Díaz, A.,
642 Martínez, A., Ratsimandresy, A., Rodríguez-Santana, A., Sangrá, P., López-Laatzen, F., Parrilla,
643 G., Pelegrí, J.L., 2002. Temporal variability of mass transport in the Canary Current. Deep-
644 Sea Res. II 49, 3415–3426.
645 Hernández-Guerra, A., Fraile-Nuez, E., Borges, R., López-Laatzen, F., Vélez-Belchí, P., Parrilla, G.,
646 Müller, T.J., 2003. Transport variability in the Lanzarote passage (Eastern Boundary Current of
647 the North Atlantic Subtropical Gyre). Deep-Sea Res. I. 50, 189–200.
648 Hernández-León, S., Gómez, M., Arístegui, J., 2007. Mesozooplankton in the Canary Current
649 System: The coastal–ocean transition zone. Prog. Oceanogr. 74(2), 397–421.
650 Hosseini-Shekarabi, S.P., Valinassab, T., Bystydzieńska, Z., Linkowski, T., 2015. Age and growth
651 of *Benthosema pterotum* (Alcock, 1890) (Myctophidae) in the Oman Sea. J. App. Ichthyol. 31,
652 51–56.
653 Hulley, P.A., 1985. Lanternfishes-Myctophidae. In: Fischer, W., Hureau, J.C., (Eds.), FAO species
654 identification sheets for fishery purposes. FAO, Southern Ocean, pp. 316–322.
655 Hulley, P.A., 1990. *Myctophidae.* In: Quero, J.C., Hureau, J.C., Karrer, C., Post, A., Saldanha, L.,
656 (Eds.). Check-list of the fishes of the eastern tropical Atlantic (CLOFETA). JNICT, Lisbon;
657 SEI; Paris; and Unesco, Paris, pp. 398–467.
658 Irigoien, X., Klevjer, T.A., Røstad, A., Martínez, U., Boyra, G., Acuña, J., Bode, A., Echevarría, F.,
659 González-Gordillo, J.I., S. Hernández-León et al., 2014. Large mesopelagic fishes biomass
660 and trophic efficiency in the open ocean. Nature Commun. 5.

661 Jørgensen, C., Holt, R.E., 2013. Natural mortality: Its ecology, how it shapes fish life histories, and
662 why it may be increased by fishing. J. Sea Res. 75, 8–18.
663 Karuppasamy, P.K., Balachandran, K., George, S., Balu, S., 2008. Food of some deep sea fishes
664 collected from the eastern Arabian Sea. J. Mar. Biol. Assoc. India. 50, 134–138.
665 Kawaguchi, K., Mauchline, J., 1982. Biology of myctophid fishes (Family Myctophidae) in the
666 Rockall Trough, northeastern Atlantic Ocean. Biol. Oceanogr. 1, 337–373.
667 Kenchington, T.J., 2014. Natural mortality estimators for information-limited fisheries. Fish. Fish.15,
668 533–562.
669 Klevjer, T. A., Irigoien, X., Røstad, A., Fraile-Nuez, E., Benítez-Barrios, V. M., Kaartvedt, S., 2016.
670 Large scale patterns in vertical distribution and behaviour of mesopelagic scattering layers.
671 Science Rep. 6.
672 Lai, H.L., Gallucci, V.F., Gunderson, D.R., Donnelly, F., Gallucci, V., Saila, S., Gustafson, D.,
673 Rothschild, B., 1996. Age determination in fisheries: methods and applications to stock
674 assessment. Stock assessment: quantitative methods and applications for small-scale fisheries,
675 pp. 82–178.
676 Linkowski, T.B., 1991. Otolith microstructure and growth patterns during the early life history of
677 lanternfishes (family Myctophidae). Can. J. Zool. 69, 1777–1792.
678 Linkowski, T.B., 1996. Lunar rhythms of vertical migrations coded in otolith microstructure of
679 North Atlantic lanternfishes, genus *Hygophum* (Myctophidae). Mar. Biol. 124, 495–508.
680 Linkowski, T.B., 1997. Morphological variation, systematics and speciation of the *Ceratoscopelus*
681 *townsendi*, *C. warmingii* complex (Osteichthyes: Myctophidae) based on the studies on the
682 morphology and microstructure of otoliths. Morski Instytut Rybacki, Gdynia. 198 pp.
683 Linkowski, T.B., Radtke, R.L., Lenz, P.H., 1993. Otolith microstructure, age and growth of two
684 species of *Ceratoscopelus* (Oosteichthyes: Myctophidae) from the eastern North Atlantic. J.
685 Exp. Mar. Biol. Ecol. 167, 237–260.
686 Longhurst, A.R., Harrison, W.G., 1989. The biological pump: profiles of plankton production and
687 consumption in the upper ocean. Prog. Oceanogr. 22, 47–123.
688 Lorenzo, J.M., Pajuelo, J.G., 1995. Biological parameters of roudi escolar *Promethichthys*
689 *prometheus* (Pisces: Gempylidae) off the Canary Islands. Fish. Res. 24, 65–71.
690 Lorenzo, J.M., Pajuelo, J.G., 1999. Biology of a deep benthopelagic fish, roudi escolar
691 *Promethichthys prometheus* (Gempylidae), off the Canary Islands. Fish. Bull. 97, 92–99.
692 Machín, F., Hernández-Guerra., A., Pelegrí, J.L., 2006. Mass fluxes in the Canary Basin. Progr.
693 Oceanogr. 70(2-4), 416–447.

McCurdy, W.J., Panfili, J., Meunier, F.J., Geffen, A.J., de Pontual, H., 2002. Preparation of calcified structures. In: Panfili, J., de Pontual, H., Troadec, H., Wright, P.J. (Eds.). Manual of Sclerochonology. Ifremer-IRD edition, Brest, pp. 331–357.

Mertz, G., Myers, R.A., 1997. Influence of errors in natural mortality estimates in cohort analysis. Can. J. Fish. Aquat. Sci. 54, 1608–1612.

Mille, T., Mahé, K., Cachera, M., Villanueva, M., de Pontual, H., Ernande, B., 2016. Diet is correlated with otolith shape in marine fish. Mar. Ecol. Progr. Ser. 555, 167–184.

Moku, M, Kawaguchi, K., 2008. Chemical composition of 3 dominant myctophid fish, Diaphus theta, Stenobrachius leucopsarus and S. nannochis in the Subarctic and transition waters of the western north Pacific. J. Mar. Biol. Assoc. UK. 88, 843–846

Moku, M., Ishimaru, K., Kawaguchi, K., 2001. Growth of larval and juvenile *Diaphus theta* (Pisces: Myctophidae) in the transitional waters of the western North Pacific. Ichthyol. Res. 48, 385–390.

Moku, M., Hayashi, A., Mori, K., Watanabe, Y., 2005. Validation of daily otolith increment formation in the larval myctophid fish *Diaphus* slender-type spp. J. Fish. Biol. 67, 1481–1485.

Morales-Nin, B., Panfili, J., 2002a. Age estimation. In: Panfili, J., de Pontual, H., Troadec, H., Wright, P.J. (Eds.). Manual of Sclerochonology. Ifremer-IRD edition, Brest, France. pp. 91–98.

Morales-Nin, B., Panfili, J., 2002b. Validation and verification methods. Indirect validation. In: Panfili, J., de Pontual, H., Troadec, H., Wright, P.J. (Eds.). Manual of Sclerochonology. Ifremer-IRD edition, Brest, France. pp. 135–137.

Mosegaard, H., Svedäng, H., Taberman, K., 1988. Uncoupling of somatic and otolith growth rates in Arctic char (*Salvelinus alpinus*) as an effect of differences in temperature response. Can. J. Fish. Aquat. Sci. 45, 1514–1524.

Moyano, M., Hernández-León, S., 2011. Intra- and interannual variability in the larval fish assemblage off Gran Canaria (Canary Islands) over 2005–2007. Mar. Biol. 158, 257–273.

Nafpaktitis, B.G., 1975. Review of the lanternfish genus Notoscopelus (family Myctophidae) in the North Atlantic and the Mediterranean. Bull. Mar. Sci. 25, 75–87.

Nafpaktitis, B.G., 1982. Myctophidae. In: Fischer, W., Bianchi, G., (eds) FAO species identification sheets for fishery purposes, 3rd edn. FAO publication, Western Indian Ocean, pp. 1–8.

Nafpaktitis, B.G., Nafpaktitis, M., 1969. Lanternfishes (Family Myctophidae) collected during cruises 3 and 6 of the R/V Anton Bruun in the Indian Ocean. Sci. Bull. Nat. Hist. Mus. Los Angeles Co. 5, 1–79.

Olivar, M.P., Hulley, P.A., Castellón, A., Emelianov, M., López, C., Tuset, V.M., Contreras, T.,

727 Molí, B., 2017. Mesopelagic fishes across the tropical and equatorial Atlantic: Biogeographical
728 and vertical patterns. Progr. Oceanogr. 151, 116-137.
729 Pajuelo, J.G., González, J.A., Santana, J.I., Lorenzo, J.M., García-Mederos, A., Tuset, V., 2008.
730 Biological parameters of the bathyal fish black scabbarfish (*Aphanopus carbo* Lowe, 1839) off
731 the Canary Islands, Central-east Atlantic. Fish. Res. 92, 140–147.
732 Pajuelo, J.G., García, S., Lorenzo, J., González, J.A., 2011. Population biology of the shark *Squalus*
733 *megalops* harvested in the central-east Atlantic Ocean. Fish. Res. 108, 31–41.
734 Pajuelo, J.G., Triay-Portella, R., Santana, J.I., González, J.A., 2015. The community of deep-sea
735 decapod crustaceans between 175 and 2600 m in submarine canyons of a volcanic oceanic island
736 (central-eastern Atlantic). Deep-Sea Res. I. 105, 83–95.
737 Pajuelo, J.G., Seoane, J., Biscoito, M., Fleitas, M., González, J.A., 2016. Assemblage of deep-sea
738 fishes on the middle slope off Northwest Africa (26º –33º N, eastern Atlantic). Deep-Sea Res.
739 I. 118, 66–83.
740 Pannella, G., 1980. Growth patterns in fish sagittae. Skeletal growth of aquatic organisms, pp. 519–
741 560.
742 Pauly, D., 1980. On the interrelationships between natural mortality, growth parameters, and mean
743 environmental temperature in 175 fish stocks. J. Con. Int. Explor. Mer. 39, 175–192.
744 Pauly, D., 1983. Length-converted catch curves, a powerful tool for fisheries research in the tropics
745 (Part I). Fishbyte, 1, 9–13.
746 Pauly, D., 1984. Length-converted catch curves: a powerful tool for fisheries research in the tropics
747 (Part II). Fishbyte, 2, 17–19.
748 Pitcher, T., MacDonald, P., 1973. Two models for seasonal growth in fishes. J. Appl. Ecol. 10, 599–
749 606.
750 Ricker, W., 1973. Linear regressions in fishery research. J. Fish. Board Can. 30, 409–434.
751 Riede, K., 2004. Global register of migratory species: from global to regional scales: final report of
752 the R&D-Projekt 808 05 081. Federal Agency for Nature Conservation.
753 Ríos, A.F., Pérez, F.F., Fraga, F., 1992. Water masses in the upper and middle North Atlantic Ocean
754 east of the Azores. Deep Sea Res. 39, 645–658.
755 Sachs, L., 1982. Applied Statistics: A Handbook of Techniques. Springer-Verlag, New York.
756 Salvanes, A., Kristoffersen, J., Steele, J., Thorpe, S., Turekian, K., 2001. Mesopelagic fish (life
757 histories, behaviour, adaptation). In: Steele J.H., Thorpe, S.A., Turekian, K.K., (Eds),
758 Encyclopedia of Ocean Sciences, Academic Press Ltd, London.
759 Sarmiento-Lezcano, A., 2016. Notes on the biology of *Notoscopelus resplendens* (Richardson, 1845)

760 off the Canary Islands. B.Sc. Thesis. Universidad de Las Palmas de Gran Canaria. 33 p.
761 Sassa C., Kawaguchi, K., Hirota, Y., Ishida. M., 2004. Distribution patterns of larval myctophid fish
762 assemblages in the subtropical-tropical waters of the western north Pacific. Fish Oceanogr. 13,
763 267–282.
764 Schindelin, J., Arganda-Carreras, I., Frise, E., Kaynig, V., Longair, M., Pietzsch, T., Preibisch, S.,
765 Rueden, C., Saalfeld, S., B. Schmid et al. 2012. Fiji: an open-source platform for biological
766 image analysis. Nat. methods. 9(7), 676–682.
767 Schnute, J., 1981. A versatile growth model with statistically stable parameters. Can. J. Fish. Aquat.
768 Sci. 38(9), 1128–1140.
769 Shelekhov, V.A., 2004. Results of otolith microstructure analysis, the growth rate, and life span of
770 *Diaphus theta* (Myctophidae). J. Ichthyo. 44, 616–623.
771 Shono, H., 2000. Efficiency of the finite correction of Akaike's Information Criteria. Fish. Sci. 66, 608–
772 610.
773 Smith, A.D., Brown, C.J., Bulman, C.M., Fulton, E.A., Johnson, P., Kaplan, I.C., Lozano- Montes, H.,
774 Mackinson, S., Marzloff, M., Shannon, L.J., Shin, Y.J., Tam, J., 2011. Impacts of fishing low–
775 trophic level species on marine ecosystems. Science 333, 1147–1150.
776 Sokal, R., Rohlf, F., 2012. Biometry, the principles and practice of statistics in biological research
777 4th edition, Freeman and Co, New York.
778 Suthers, I.M., 1996. Spatial variability of recent otolith growth and RNA indices in pelagic juvenile
779 *Diaphus kapalae* (Myctophidae): an effect of flow disturbance near an island? Mar. Freshw.
780 Res. 47(2), 273–282.
781 Sutton, T., Clark, T., Dunn, M.R., Halpin, D.C., Rogers, P.N., Guinotte, A.D., et al, 2017. A global
782 biogeographic classification of the mesopelagic zone. Deep-Sea Res. I. 126, 85–102.
783 Takagi, K., Yatsu, A., Moku, M., Sassa, C., 2006. Age and growth of lanternfishes, *Symbolophorus*
784 *californiensis* and *Ceratoscopelus warmingii* (Myctophidae), in the Kuroshio–Oyashio
785 Transition Zone. Ichthyol. Res. 53, 281–289.
786 Watanabe H., Moku, M, Kawaguchi K., Ishimaru, K., Ohno, A., 1999. Diel vertical migration of
787 myctophid fishes (Family Myctophidae) in the transitional waters of the western North Pacific.
788 Fish Oceanogr. 8, 115–127
789 Wilke, I., Meggersb, H., Bickertcet. T., 2009. Depth habitats and seasonal distributions of recent
790 planktic foraminifers in the Canary Islands region (29°N) based on oxygen isotopes. Deep-Sea
791 Res. I 56, 89–106,
792 Williams, E.H., Shertzer, K.W., 2003. Implications of life-history invariants for biological reference

points used in fishery management. Can. J. Fish. Aquat. Sci. 60, 710–720.
Winemiller, K.O., Rose, K.A., 1992. Patterns of life-history diversification in North American fishes: implications for population regulation. Can. J. Fish. Aquat. Sci. 49, 2196–2218.
Yatsu, A., Sassa, C., Moku, M., Kinoshita, T., 2005. Night-time vertical distribution and abundance of small epipelagic and mesopelagic fishes in the upper 100 m layer of the Kuroshio–Oyashio Transition Zone in Spring. Fish. Sci. 71, 1280–1286.
Young, J.W., Bulman, C.M., Blaber, S.J.M., Wayte, S.E., 1988. Age and growth of the lanternfish *Lampanyctodes hectoris* (Myctophidae) from eastern Tasmania, Australia. Mar. Biol. 99, 569–576.

Figure captions

Figure 1. Location of the Canary Islands and sampling area conducted by the B/E "*La Bocaina*" between 1999 and 2002.

Figure 2. Lateral view of the distal and proximal surface of the right otolith of *Notoscopelus resplendens* off the Canary Islands. Omd minimum diameter, OMd maximum diameter and r radius. D, dorsal plane; V, ventral plane; A, anterior plane, P posterior plane.

Figure 3. Length-weight relationships by sexes of *Notoscopelus resplendens* off the Canary Islands.

Figure 4. Temperature and salinity profiles from 0 to 500 m depth off the Canary Islands. Dashed lines (February, lowest vertical diel range) continuous lines (September, highest vertical diel range).

Figure 5. Otolith maximum diamiter (OMd)-standard length (down), and otolith minimum diameter (Omd)-standard length relationships (up) by sexes of *Notoscopelus resplendens* off the Canary Islands.

Figure 6. Pattern of the increment formation for otoliths with 0 to 4 translucent rings. R is the mean size (±SD) of the otoliths with 1 to 4 translucent rings of *Notoscopelus resplendens* off the Canary Islands.

Figure 7. Picture composition of a Sagittal otoliths section of a 1 years-old (310 daily growth increments) specimen of *Notoscopelus resplendens* off the Canary Islands (SL= 91.2 mm).

Figure 8. Picture composition of 139 daily growth increment in an otolith of N*otoscopelus resplendens* off the Canary Islands. LZ, larval zone; PZ, Postlarval zone and PMZ, Postmetamorphic zone.

Figure 9. Age bias plot for readers 1 and 2 ageing all otoliths of N*otoscopelus resplendens* off the Canary Islands. Each error bar represents the standard deviation. The 1:1 equivalence (solid line) is also indicated.

Figure 10. Gompertz (up) and von Bertalanffy growth (down) curves for males and females of *Notoscopelus resplendens* off the Canary Islands.

Figure 11. Gompertz curves for otolith weight-age relationship for males and females of *Notoscopelus resplendens* off the Canary Islands.

Figure 12. Values of the natural mortality obtained from age and length frequency data, and from empirical equations reviewed by Kenchington (2014) for *Notoscopelus resplendens* off the Canary Islands.

Table 1. Mean length by age class for males, females and all fish of *Notoscopelus resplendens* off the Canary Islands. N is the number of fish by age class. S.D. is the Standard deviation.

	Total		Males		Females	
Age (years)	N	Mean length ± S.D. (mm)	N	Mean length ± S.D. (mm)	N	Mean length ± S.D. (mm)
0	71	27.44± 5.35	3	30.96±2.39	5	32.86±1.87
I	144	40.70±5.02	62	41.05±5.70	21	40.58±6.15
II	49	63.28±6.63	26	61.86±7.29	23	64.90±5.52
III	56	73.37±3.73	26	73.56±3.55	30	73.21±3.92
IV	20	77.49±3.21	12	77.59±3.66	8	77.34±2.61

Table 2. Growth parameters estimates and model selection criterion for male and female of *Notoscopelus resplendens*. L_{∞}, theoretical asymptotic length; k, growth coefficient; t_0, theoretical age at zero length; C, the amplitude of the fluctuation in seasonal growth; ts, the addition of the point of the minimum growth + 0.5. y_1, the estimated mean length of the smallest age individuals in the sample; y_2, the estimated mean length of the largest age individuals in the sample; a and b, model parameters; A_w, Akaike weights.

Model/ parameters	Males	Females
	Estimates (±S.D.)	Estimates (±S.D.)
von Bertalanffy growth model		
L_{∞} (mm)	93.054 (5.089)	90.85 (6.297)
k (year^{-1})	0.455 (0.072)	0.493 (0.104)
t_0 (year)	0.003 (0.115)	-0.059 (0.164)
R^2	0.912	0.839
A_w	0.39	0.39
Seasonalised von Bertalanffy growth model		
L_{∞} (mm)	95.003 (5.621)	95.20 (9.327)
k (year^{-1})	0.427 (0.070)	0.407 (0.090)
t_0 (year)	-0.049 (0.120)	-0.168 (0.242)
C	0.243 (0.193)	0.240 (0.195)
ts	0.226 (0.188)	0.297 (0.187)
R^2	0.899	0.816
A_w	0.02	>0.001
Gompertz growth model		
L_{∞} (mm)	85.940 (2.919)	86.347 (3.615)
k (year^{-1})	0.740 (0.076)	0.799 (0.114)
t_0 (year)	0.888 (0.041)	0.902 (0.069)
R^2	0.915	0.845
A_w	0.41	0.45
Schnute growth model		
y_1 (mm)	26.569 (2.024)	27.736 (2.809)
y_2 (mm)	79.795 (1.543)	78.119 (1.542)
a	2.359 (1.097)	2.497 (0.660)
b	-5.236 (3.363)	-5.512 (0.331)
R^2	0.910	0.826
A_w	0.17	0.16

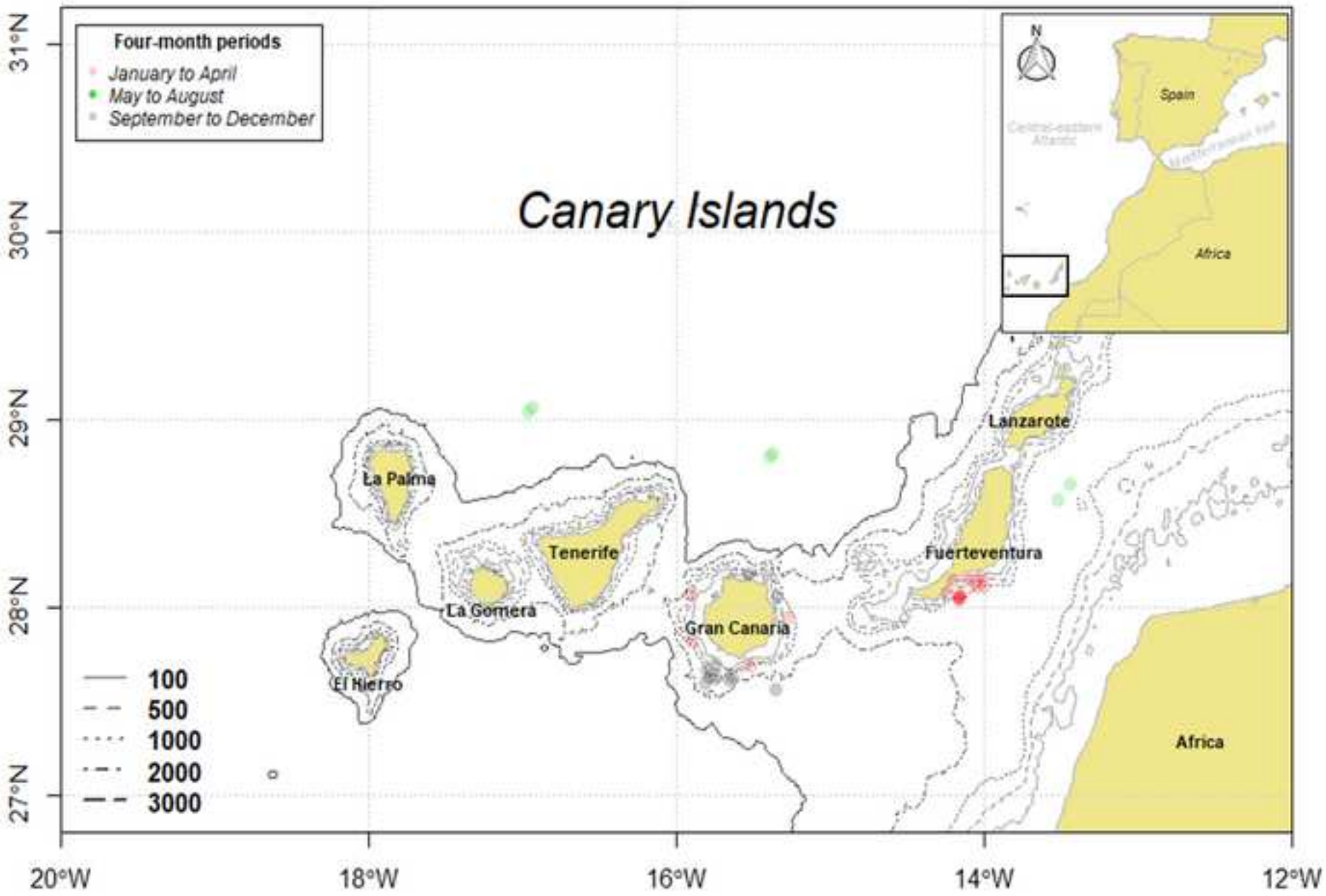
Four-month periods
January to April
May to August
September to December
Canary Islands
N
Spain
Africa
Lanzarote
Fuerteventura
La Palma
Tenerife
La Gomera
Gran Canaria
El Hierro
Africa
100
500
1000
2000
3000
31°N
30°N
29°N
28°N
27°N
20°W
18°W
16°W
14°W
12°W

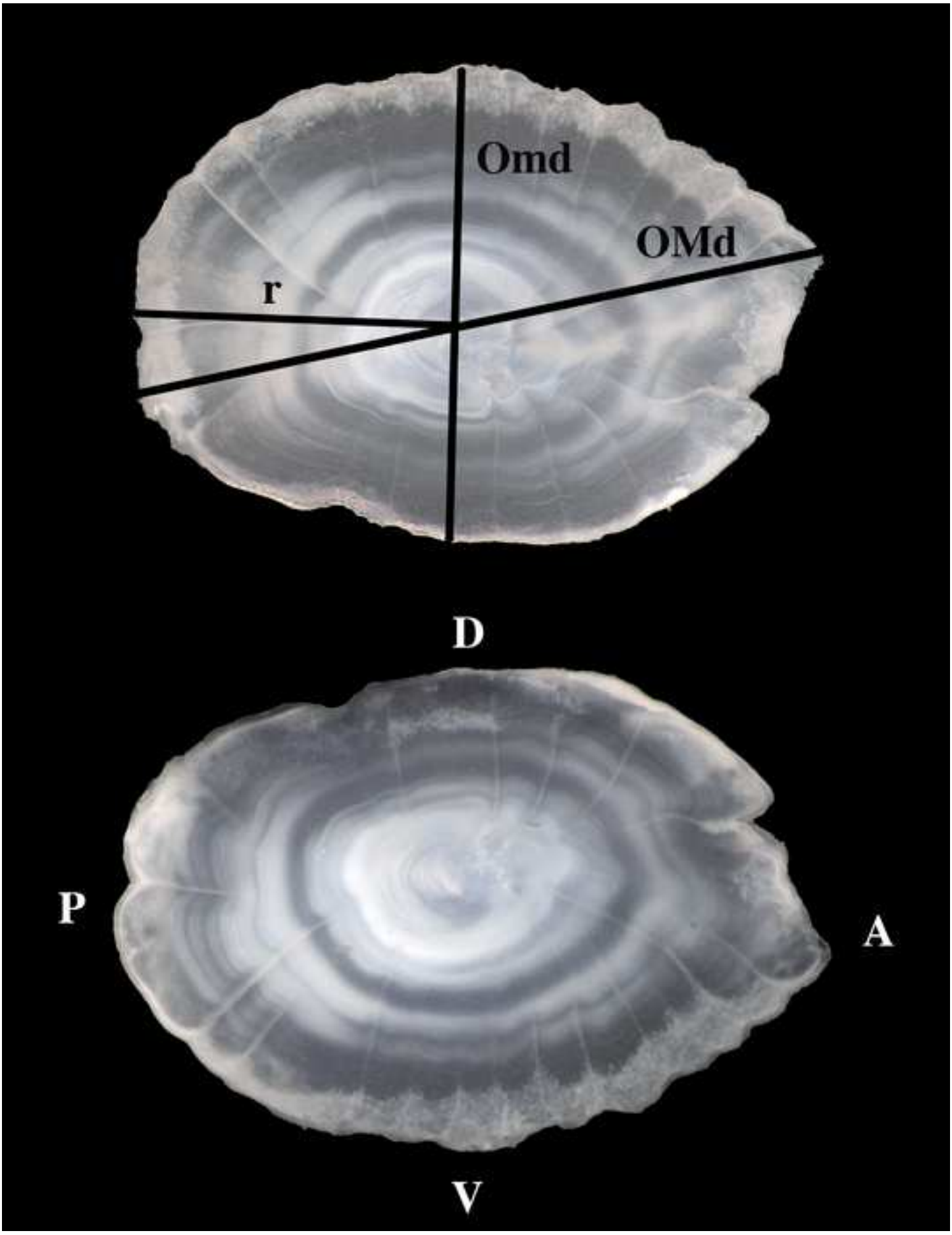
Omd
OMd
r
D
P
A
V

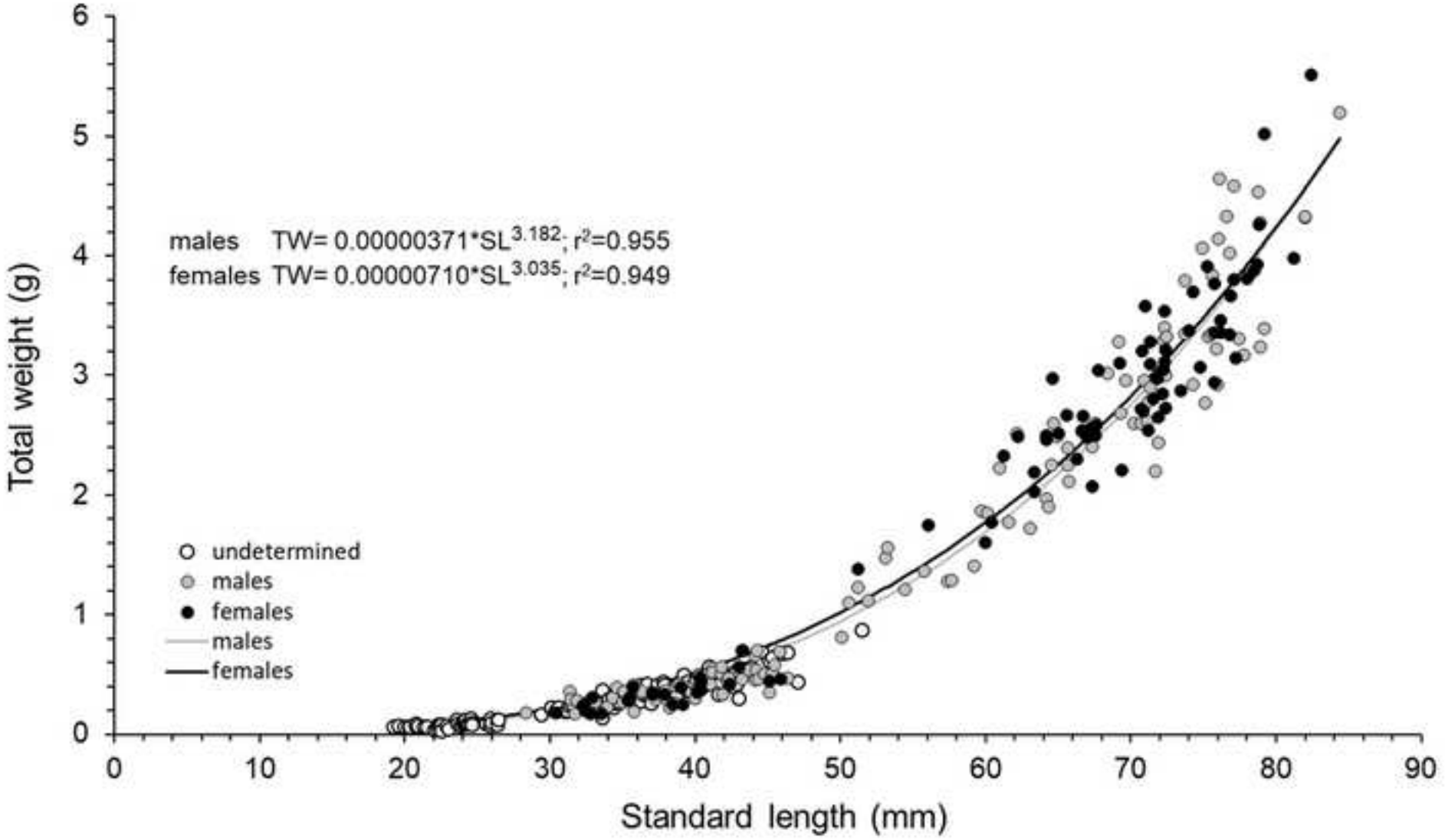
males TW= 0.00000371*SL3.182; r2=0.955
females TW= 0.00000710*SL3.035; r2=0.949
undetermined
males
females
males
females
Total weight (g)
Standard length (mm)
0
1
2
3
4
5
6
0
10
20
30
40
50
60
70
80
90

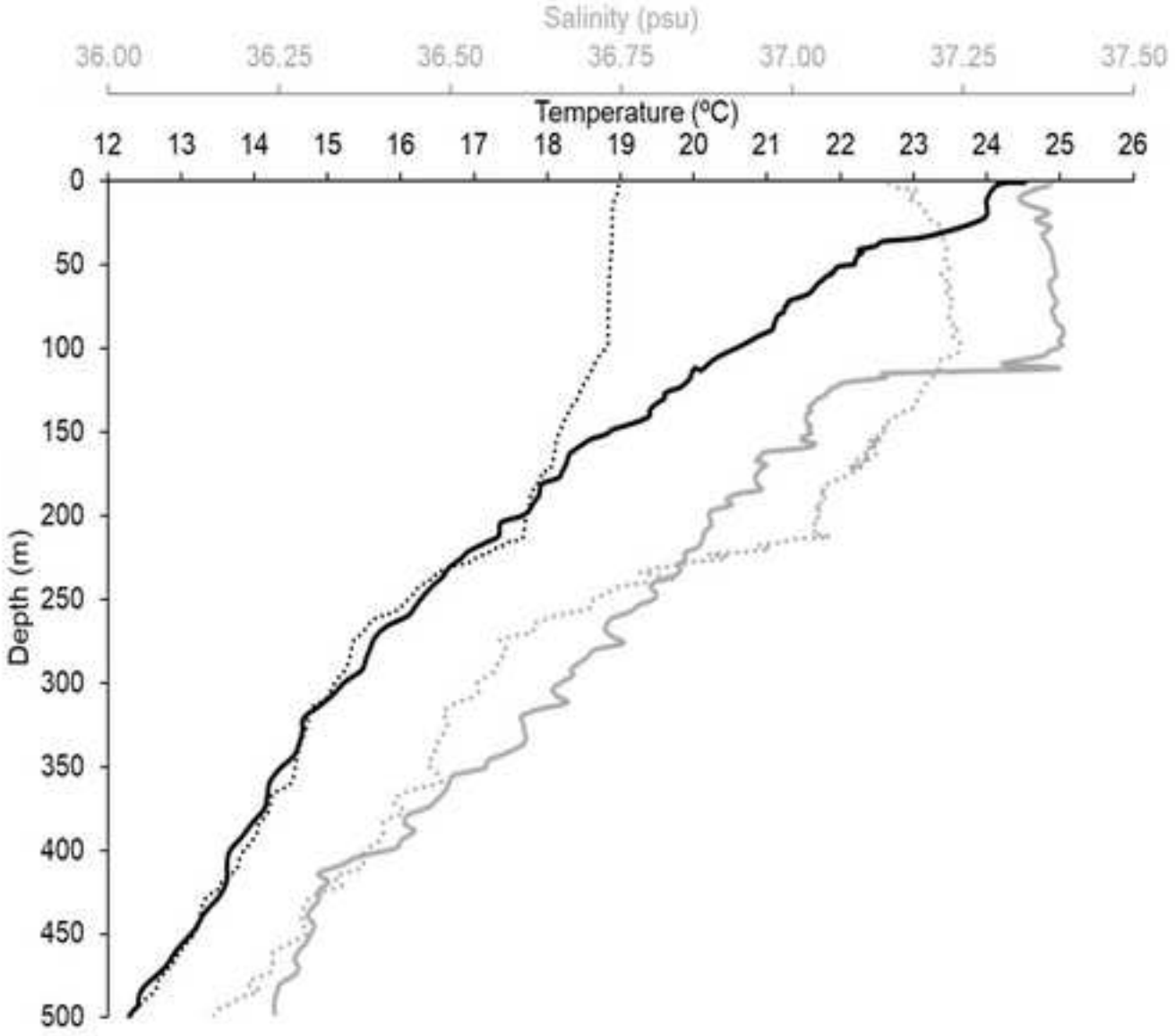
Salinity (psu)
36.00
36.25
36.50
36.75
37.00
37.25
37.50
Temperature (°C)
12
13
14
15
16
17
18
19
20
21
22
23
24
25
26
Depth (m)
0
50
100
150
200
250
300
350
400
450
500

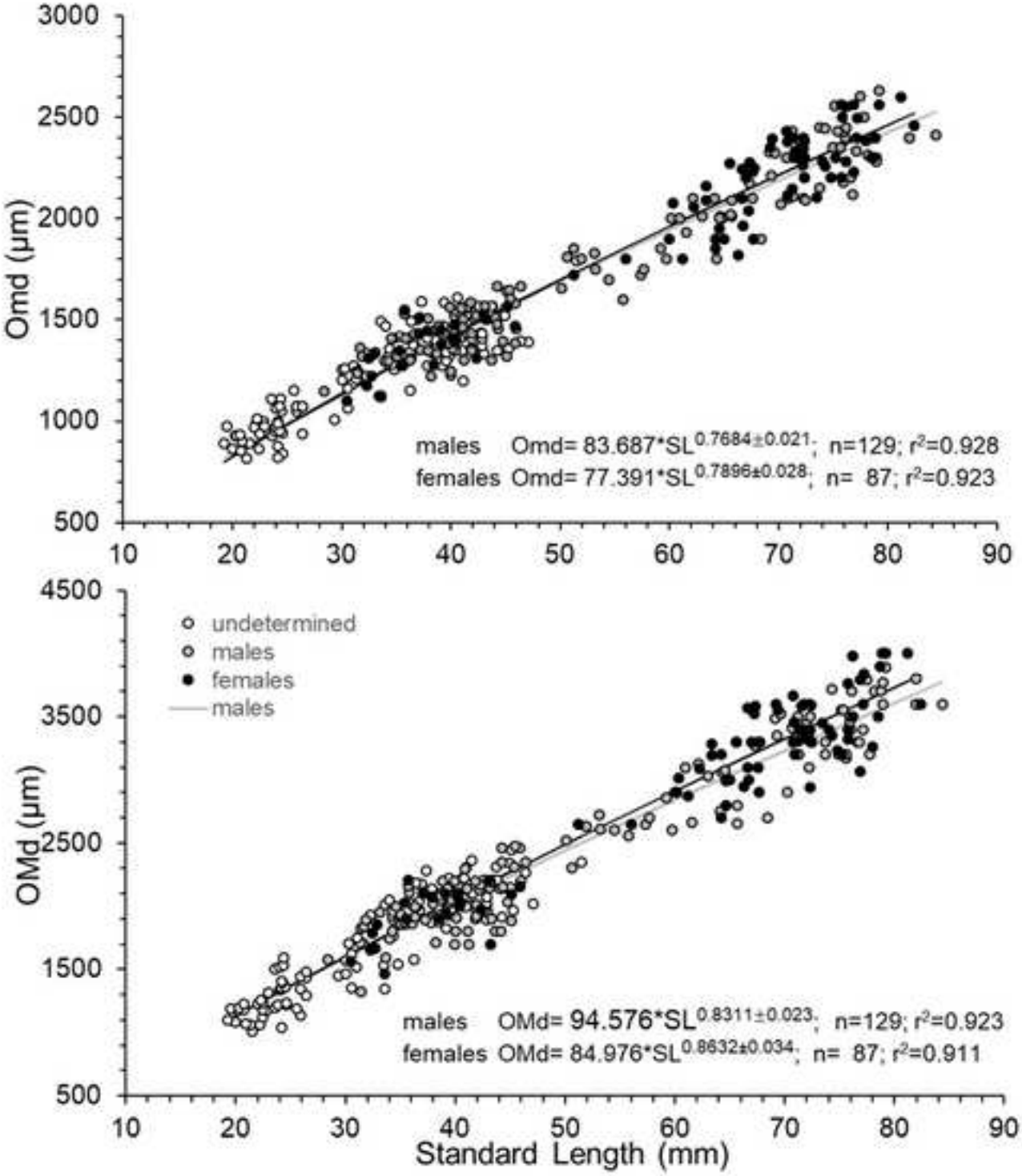
Omd (µm)
3000
2500
2000
1500
1000
500
10
20
30
40
50
60
70
80
90
males Omd= 83.687*SL^0.7684±0.021; n=129; r²=0.928
females Omd= 77.391*SL^0.7896±0.028; n= 87; r²=0.923
undetermined
males
females
males
OMd (µm)
4500
3500
2500
1500
500
males OMd= 94.576*SL^0.8311±0.023; n=129; r²=0.923
females OMd= 84.976*SL^0.8632±0.034; n= 87; r²=0.911
Standard Length (mm)

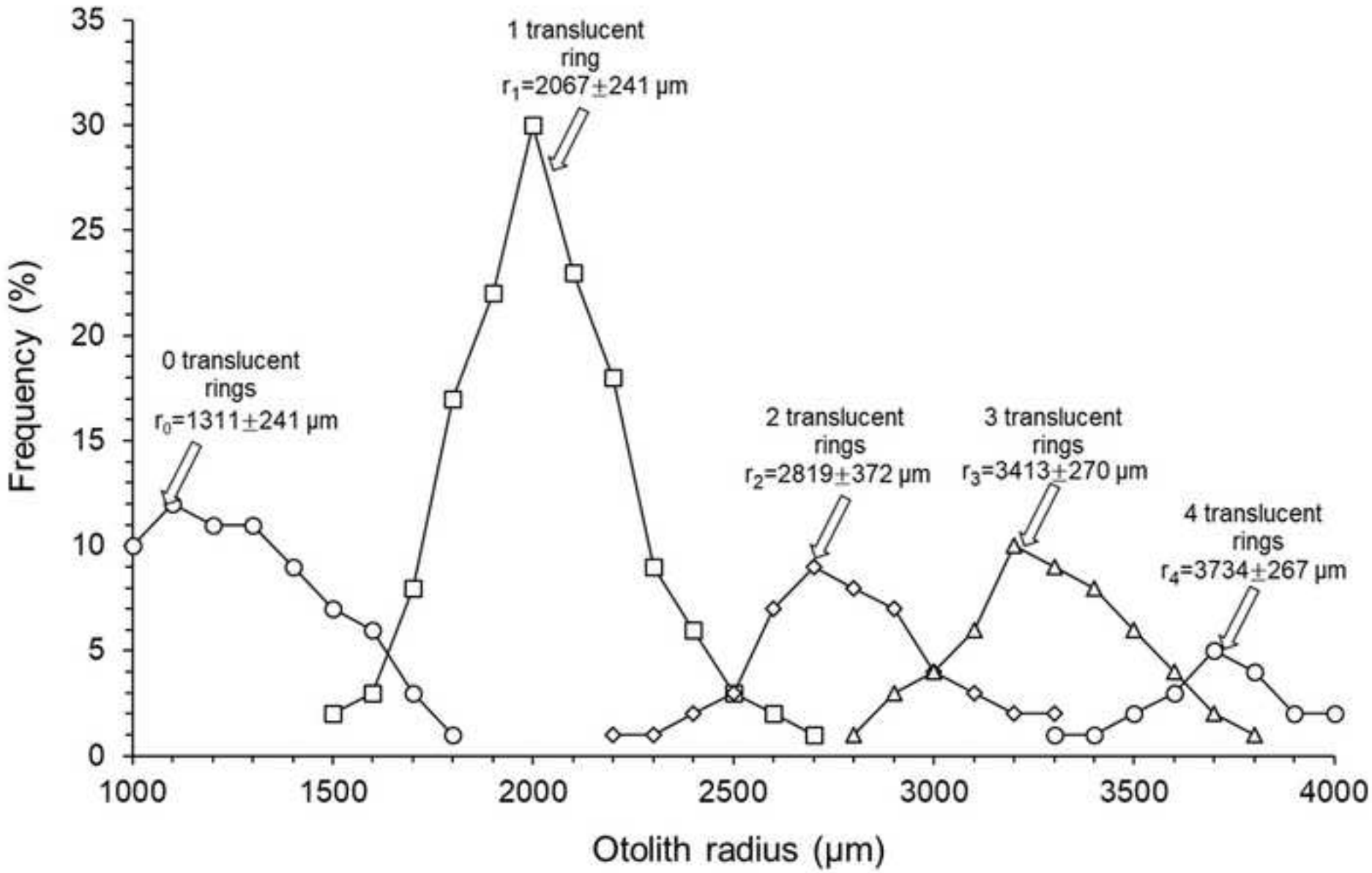
35
30
25
20
15
10
5
0
Frequency (%)
1000
1500
2000
2500
3000
3500
4000
Otolith radius (μm)
0 translucent rings
r0=1311±241 μm
1 translucent ring
r1=2067±241 μm
2 translucent rings
r2=2819±372 μm
3 translucent rings
r3=3413±270 μm
4 translucent rings
r4=3734±267 μm

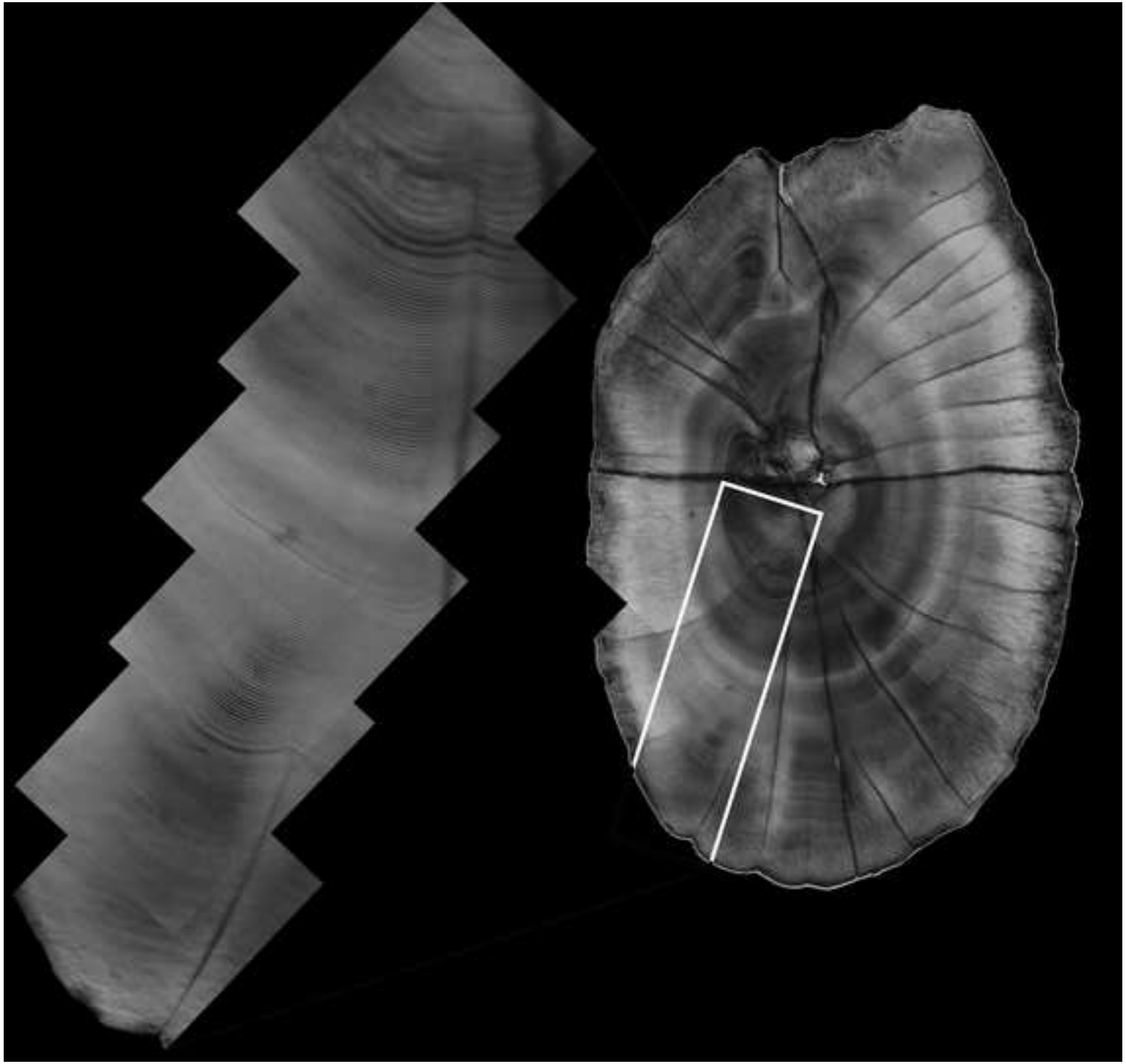

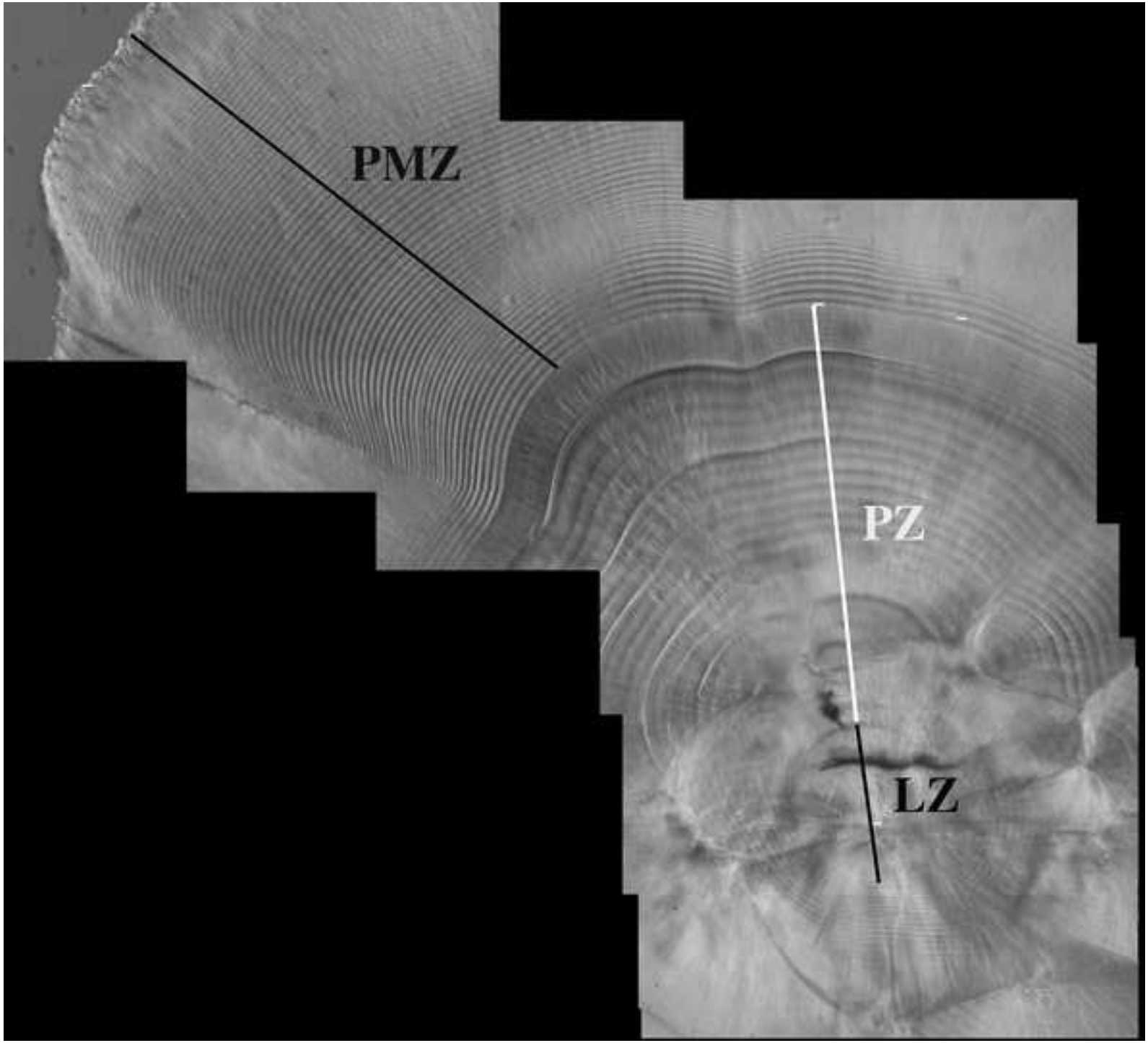
PMZ
PZ
LZ

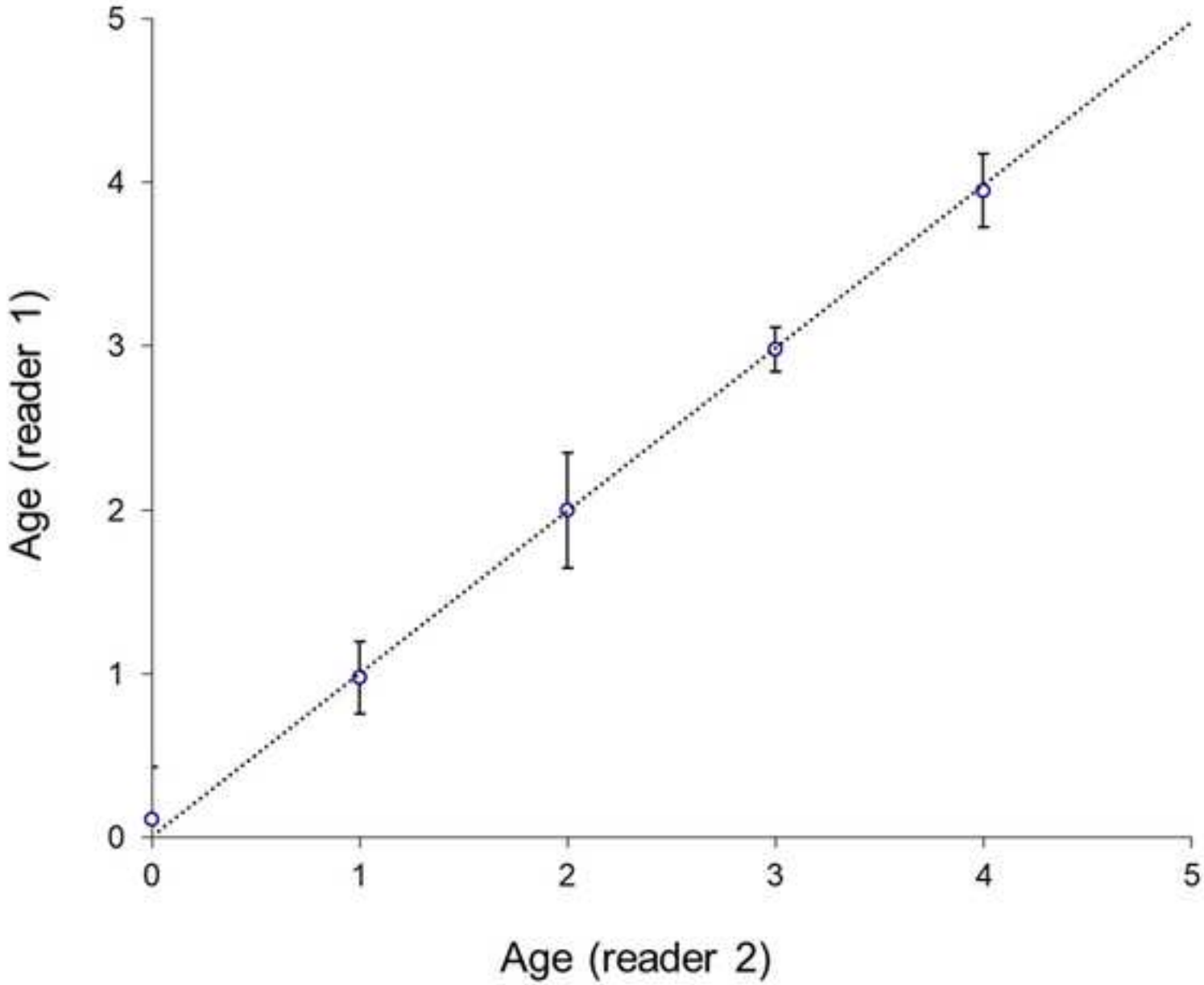
Age (reader 1)
Age (reader 2)
0
1
2
3
4
5

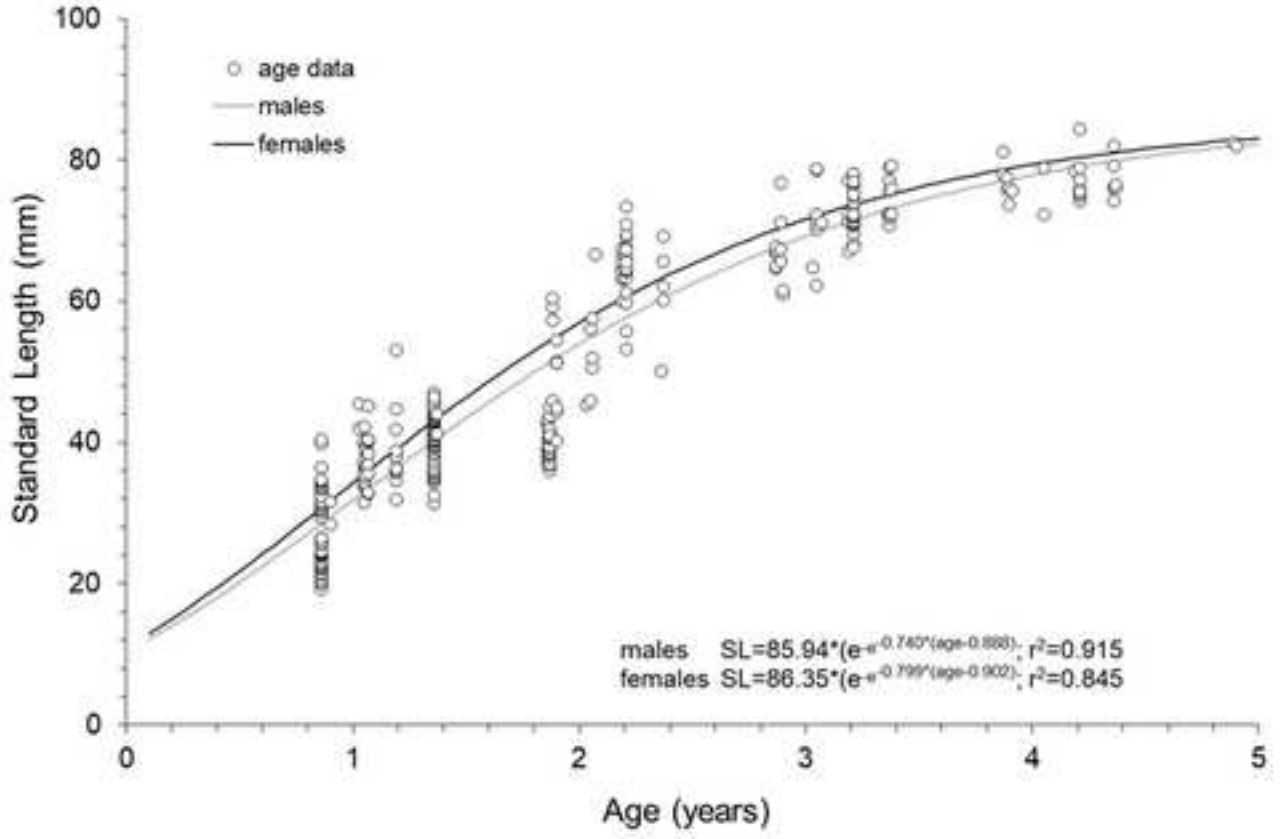
age data
males
females
Standard Length (mm)
Age (years)
males SL=85.94*(e-e-0.740*(age-0.888)); r2=0.915
females SL=86.35*(e-e-0.799*(age-0.902)); r2=0.845

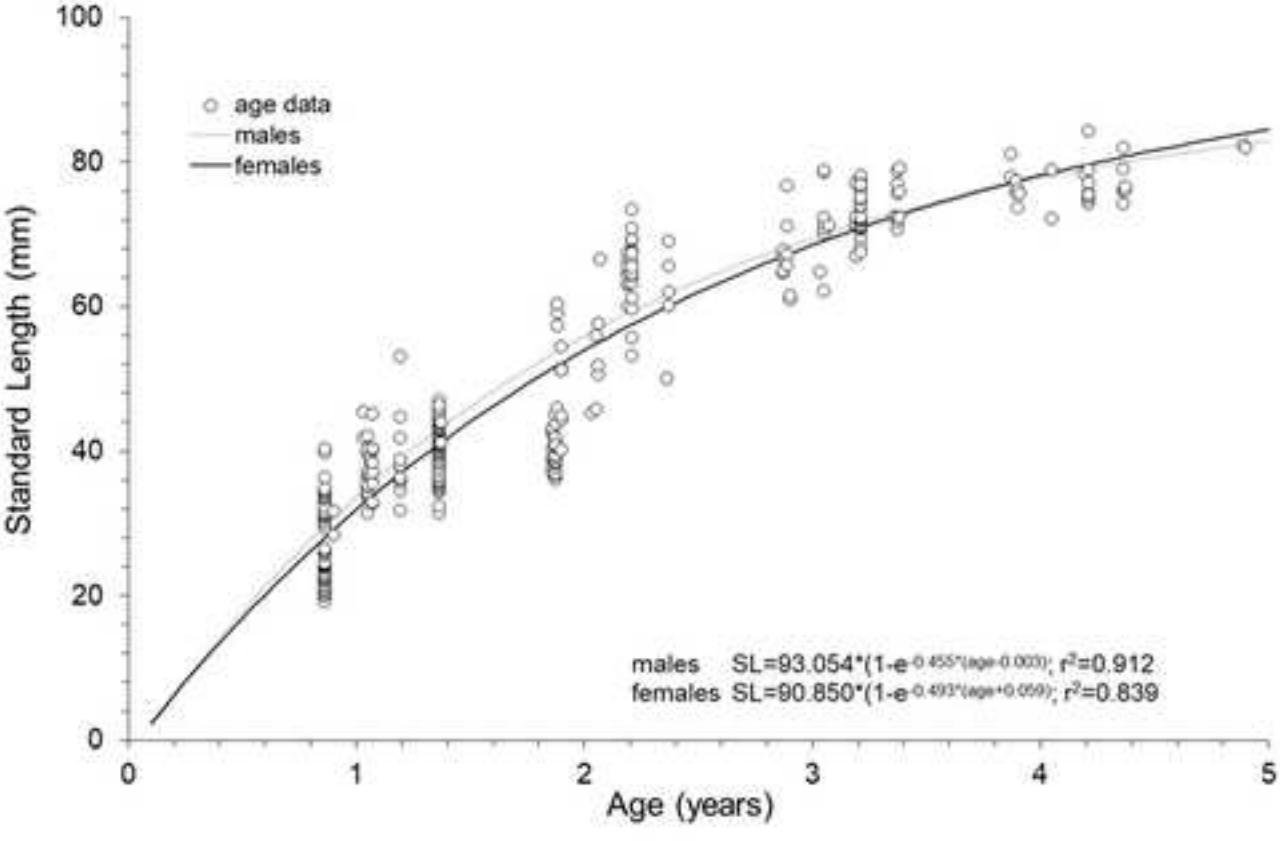
age data
males
females
Standard Length (mm)
Age (years)
males SL=93.054*(1-e-0.455*(age-0.003)); r2=0.912
females SL=90.850*(1-e-0.493*(age+0.059)); r2=0.839

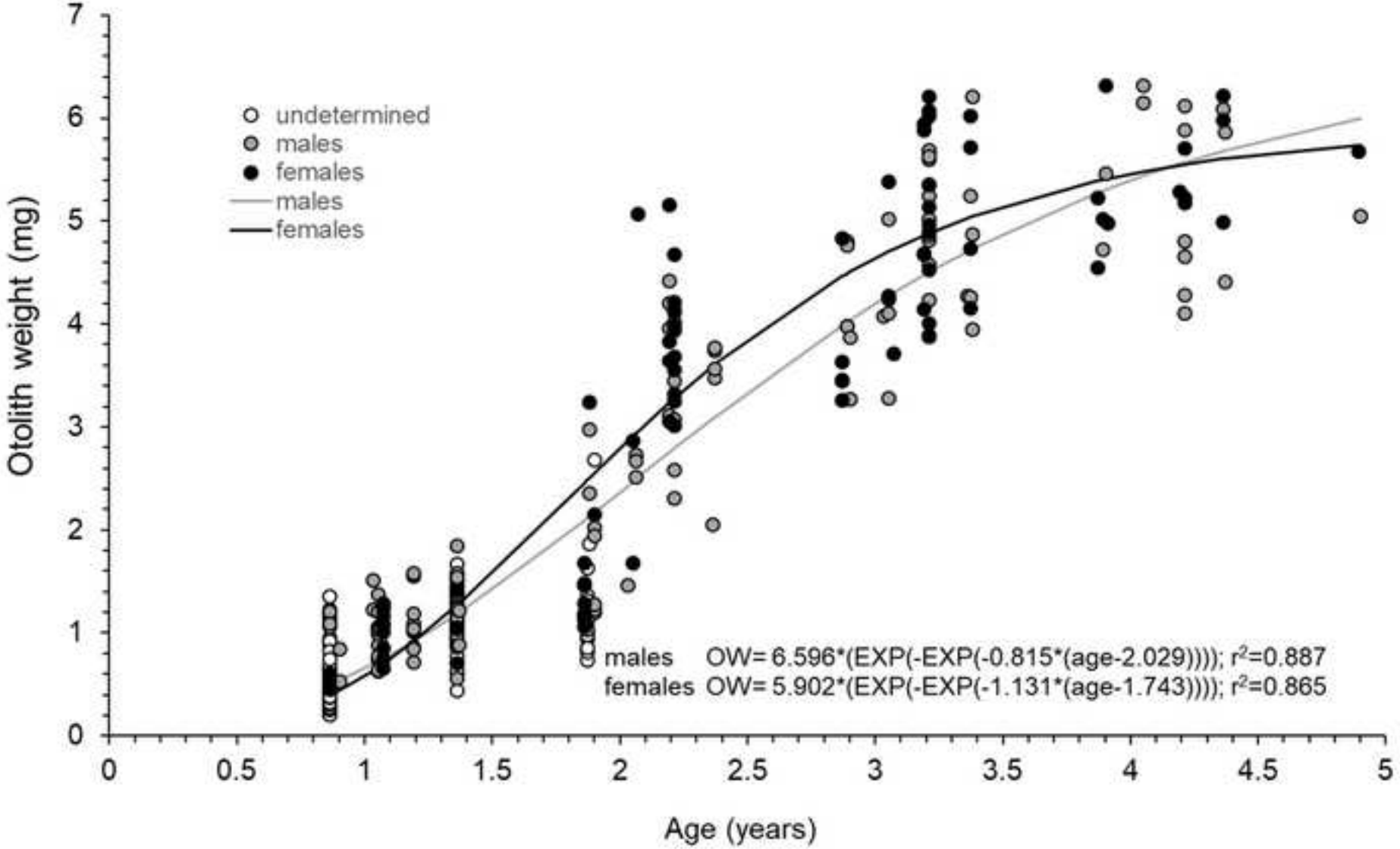
undetermined
males
females
males
females
Otolith weight (mg)
Age (years)
0
1
2
3
4
5
6
7
0
0.5
1
1.5
2
2.5
3
3.5
4
4.5
5
males OW= 6.596*(EXP(-EXP(-0.815*(age-2.029)))); r2=0.887
females OW= 5.902*(EXP(-EXP(-1.131*(age-1.743)))); r2=0.865

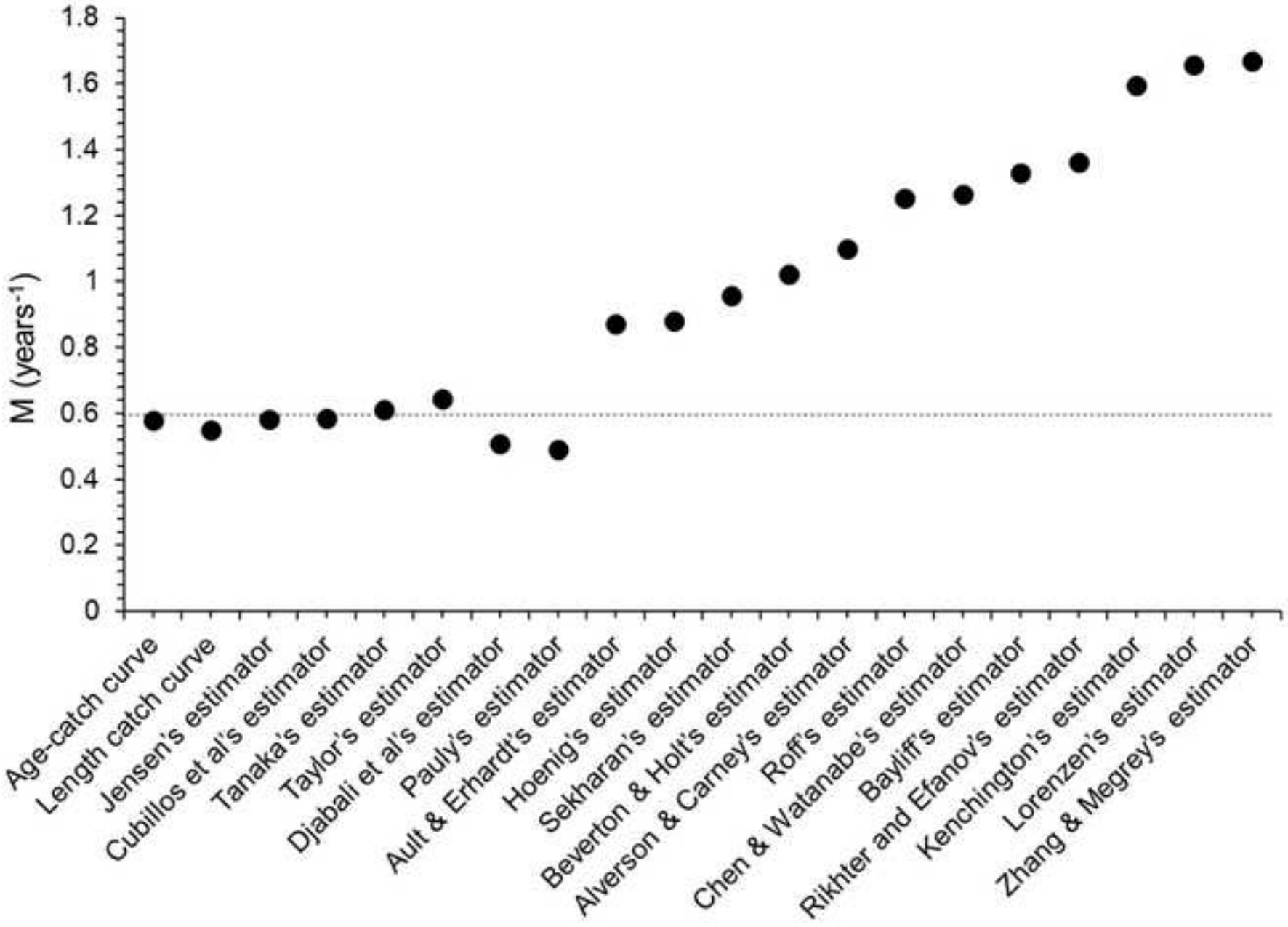
M (years-1)
1.8
1.6
1.4
1.2
1
0.8
0.6
0.4
0.2
0
Age-catch curve
Length catch curve
Jensen's estimator
Cubillos et al's estimator
Tanaka's estimator
Taylor's estimator
Djabali et al's estimator
Pauly's estimator
Ault & Erhardt's estimator
Hoenig's estimator
Sekharan's estimator
Beverton & Holt's estimator
Alverson & Carney's estimator
Roff's estimator
Chen & Watanabe's estimator
Bayliff's estimator
Rikhter and Efanov's estimator
Kenchington's estimator
Lorenzen's estimator
Zhang & Megrey's estimator